Sensors & Diagnostics

CRITICAL REVIEW

View Article Online
View Journal | View Issue

Cite this: *Sens. Diagn.*, 2025, **4**, 111

The development of GFETs for biometric applications

Weisong Yang,[a] Weihao Feng,[a] Siyu Hou,[a] Zhuang Hao,[b] Cong Huang[ac] and Yunlu Pan *[a]

Due to the rising prevalence of chronic diseases worldwide attributed to an aging population and the development of big data and artificial intelligence (AI), there is a significant demand for healthcare and long-term disease monitoring. As an emerging sensing technology, graphene field-effect transistor (GFET) sensors are anticipated to become the backbone of future large-scale electronic applications, owing to their rapid and accurate disease diagnosis capabilities, excellent biocompatibility, and ease of system integration. This review summarizes the recent advances in biosensing applications using GFETs. Initially, the working mechanism of GFETs for biosensing is briefly introduced, followed by an outline of various gate configuration strategies employed in GFETs and a discussion on methods for enhancing sensing performance. The multiplexing capabilities and flexible wearable applications of GFETs are then summarized and highlighted, aiming to increase the diversity and applicability of these sensors. Subsequently, a comprehensive survey of the advancements in the integration and miniaturization of multi-component GFET biosensors is discussed. Moreover, this review provides an outlook on the challenges and prospects associated with the commercialization of GFET technology in the biosensing field.

Received 25th September 2024,
Accepted 22nd November 2024

DOI: 10.1039/d4sd00317a

rsc.li/sensors

[a] *State Key Laboratory of Robotics and Systems, School of Mechatronics Engineering, Harbin Institute of Technology, Harbin 150001, China. E-mail: yunlupan@hit.edu.cn*
[b] *School of Mechanical Engineering & Automation, Beihang University, Beijing 100191, China*
[c] *Chongqing Research Institute of Harbin Institute of Technology, Chongqing, 401151, China*

1. Introduction

In recent decades, the intersection of the escalating global trend towards an aging population and the rapid advancements in big data and AI has generated a significant demand in the market for digital healthcare and disease prevention.[1–3] Numerous emerging sensing and detection technologies have been progressively developed and applied,

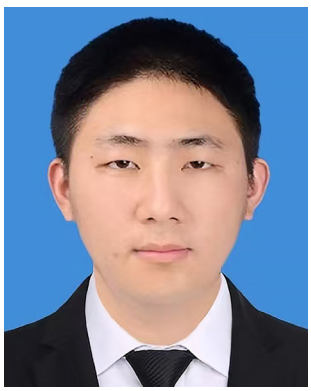

Weisong Yang

Weisong Yang is currently a PhD candidate at the State Key Laboratory of Robotics and Systems, School of Mechatronics Engineering, Harbin Institute of Technology. His research focuses on flexible wearable biosensors made of 2D materials for early disease diagnosis and personal health care. He received his Bachelor of Engineering degree and Master of Engineering degree in Mechanical Engineering from Harbin Institute of Technology, China. After the postgraduate study, he started his PhD at the State Key Laboratory of Robotics and Systems in 2023.

Weihao Feng

Weihao Feng is currently a Master's student at the State Key Laboratory of Robotics and Systems, School of Mechatronics Engineering, Harbin Institute of Technology. His research focuses on the application of graphene biosensors for daily physiological monitoring applications. He received his Bachelor's degree in Mechanical Engineering (2019) from Taiyuan University of Technology, China, and continued his education at Harbin Institute of Technology to pursue a Master's degree in Mechanical Engineering in 2023.

encompassing methodologies such as enzyme-linked immunosorbent assay (ELISA),[4,5] electrochemical impedance spectroscopy (EIS),[6–8] surface-enhanced Raman spectroscopy (SERS),[9–11] and field-effect transistor (FET) sensors,[12–15] among others. Simultaneously, graphene, a single-atom-thick two-dimensional (2D) nanomaterial renowned for its distinctive electrical properties, has garnered substantial attention.[16,17] Given its inherent attributes, including high carrier mobility, elevated carrier saturation drift speed, and significant Young's modulus,[18–20] graphene has seen notable advancements in its application in FET sensors. Particularly, GFET sensors boast advantages such as label-free operation, high sensitivity, rapid response, and a convenient detection procedure.[21–24]

At the beginning, GFET sensors are mainly built on rigid substrates such as SiO_2, often using liquid gate control with an external gate or a flat gate for biosensing.[25–28] In pursuit of enhanced detection performance and efficiency, innovative gate configuration structures, including the back gate and floating gate, have been explored for integration into GFETs.[29–31] However, the ductility and flexibility of traditional rigid GFET sensors are limited, making it difficult for them to continuously adhere to the surface of human skin, which poses several limitations in daily life.[32–35] Secondly, the detection objects of sensors also need to be diversified to meet the needs of people in digital healthcare and disease prevention. A variety of flexible materials are used in GFET sensors, along with the integration of digital communication technologies. This enables the sensors to achieve both multiplexing and flexible, wearable applications.[12,36–40] Compared to the large size and rigidity of traditional electronic products, wearable devices are lightweight, flexible, and cost-effective, and can further maintain conformal contact with a wide range of human skin types, improving patient compliance and expanding the application range of GFET sensors.[41–43]

This article provides an overview of recent advances in detecting biomarkers using GFETs, as depicted in Fig. 1. We commence with a brief comparison comparing the two working mechanisms of GFETs for biosensing, followed by an analysis of the various gate configuration strategies employed in GFETs, including external Ag/AgCl gate, planar gate, back gate, top gate, and floating gate configurations, to elucidate ways to improve sensing performance. Then, the

Siyu Hou

Siyu Hou is currently a Master's student at the State Key Laboratory of Robotics and Systems, School of Mechatronics Engineering, Harbin Institute of Technology. Her research focuses on miniaturization and portability of biosensors made of 2D materials for environmental monitoring. She received her Bachelor's degree (2022) in Mechanical Engineering from Harbin Institute of Technology and continued her research at the State Key Laboratory of Robotics and Systems in 2023.

Zhuang Hao

Dr Zhuang Hao is an Associate Professor at the School of Mechanical Engineering & Automation, Beihang University. His research focuses on highly integrated portable devices and flexible wearable MEMS/NEMS biosensors, and photoelectric sensor devices based on low-dimensional nano-material transducers.

Cong Huang

Dr Cong Huang is currently a post-doctoral researcher at the School of Mechatronics Engineering, Harbin Institute of Technology. He received his Ph. D. degree from the State Key Laboratory of Robotics and Systems, Harbin Institute of Technology, China in 2022. His research focuses on wearable electronics and flexible biosensors.

Yunlu Pan

Dr Yunlu Pan is currently a Professor at the School of Mechatronics Engineering, Harbin Institute of Technology. His current research interests include the processing and application of super-infiltrated surfaces and low-dimensional material-based sensing testing techniques. He has published over 40 SCI papers in the last five years, and his H index is 32.

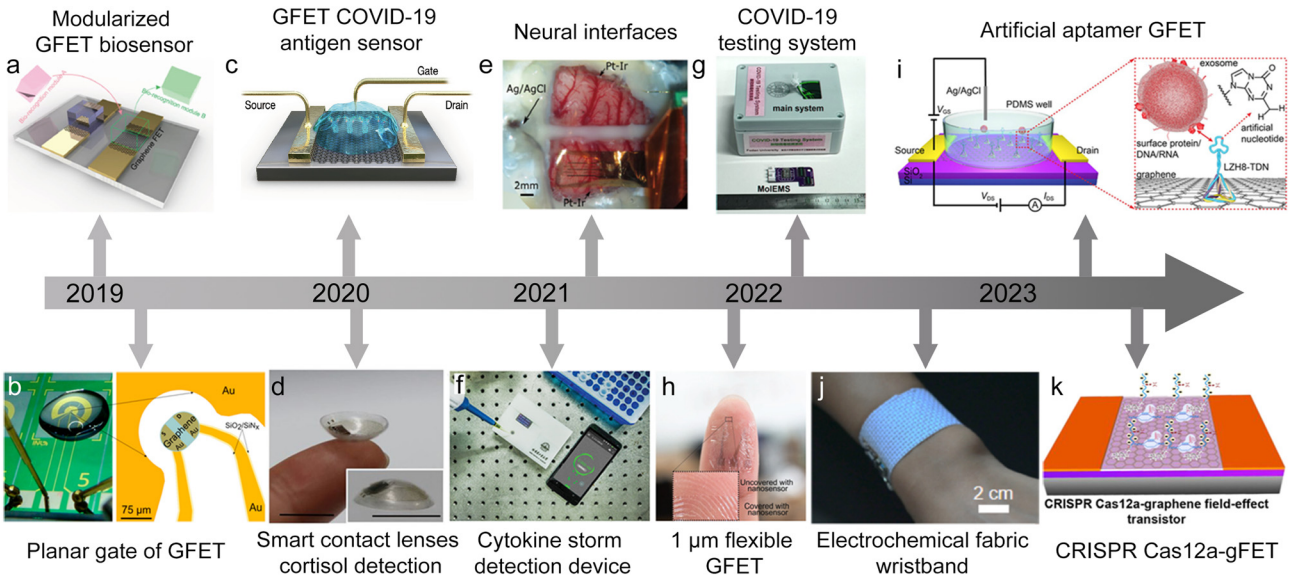

Fig. 1 The development of a GFET for biosensing applications. a) Modular concept of a GFET biosensor. Reproduced with permission.[44] Copyright 2019, *Nano Letters*. b) Optical image of a planar transistor chip. Reproduced with permission.[45] Copyright 2019, *ACS Sensors*. c) GFET COVID-19 antigen sensor. Reproduced with permission.[26] Copyright 2020, *ACS Nano*. d) Smart contact lens sensor. Reproduced with permission.[37] Copyright 2020, *Science Advances*. e) Neural sensing interface based on a GFET. Reproduced with permission.[43] Copyright 2021, *Nature Communications*. f) An integrated device for cytokine detection. Reproduced with permission.[36] Copyright 2021 *Small*. g) An integrated device for COVID-19 testing. Reproduced with permission.[39] Copyright 2022, *Nature Biomedical Engineering*. h) A flexible GFET consisting of a 1 μm polymer substrate. Reproduced with permission.[46] Copyright 2022, *Advanced Materials Technologies*. i) A type of artificial nucleotide aptamer sensor. Reproduced with permission.[47] Copyright 2023, *Analytical Chemistry*. j) Demonstration of an electrochemical fabric: wristband. Reproduced with permission.[48] Copyright 2023, *Biosensors and Bioelectronics*. k) CRISPR Cas12a-gFET biosensor array. Reproduced with permission.[49] Copyright 2023, *ACS Sensors*.

multiplexing capability of GFETs is analysed, wherein different devices detect the same biological signal or multiple modules in a single device detect multiple biomarkers simultaneously. Additionally, the methods of achieving flexible and lightweight wearable applications are analysed, aiming to enhance the diversity and applicability of these sensors. The focus then transitions to the progress of GFET technology in the miniaturization and portability of biomonitoring prototypes. Finally, our discussion synthesizes the potential prospects and challenges associated with GFET technology in the realms of healthcare, wearable electronics, and other applications.

2. Working mechanism of GFETs

GFET sensors are commonly configured in either a liquid-gated or back-gated arrangement. In liquid-gated GFET sensors, the gate is usually immersed in solution and the gate voltage is applied on top of the graphene. The coupling between the gate and the graphene channel takes place through the interface capacitor C, which comprises an electric double layer (EDL) capacitor C_{DL} and a quantum capacitor C_Q of graphene established at the solution-to-graphene interface, as depicted in Fig. 2a.[50–52]

While biomolecules as a whole are generally considered electrically neutral, specific structural regions may exhibit positive or negative behaviour, behaving as charged ions when adsorbed on the graphene surface. Two distinct physical processes are employed to elucidate how a biomolecular move to the surface of graphene induces changes in conductivity. The first process, known as charge transfer to the graphene surface causing doping, involves the adsorption of ions as dopants, facilitating the exchange of electrons into or out of the graphene. The second method involves charge induction, which causes the capacitance of the EDL capacitor to change, resulting in a change in the potential of the electrolyte.[57,58] This potential change induces charge accumulation on the graphene surface, consequently altering the carrier density of graphene.

2.1 Electron exchange theory

Special attention should be paid to the charge shielding due to the Debye length (λ_D) under solution detection conditions. When tested in an electrolyte environment, it is crucial to control the binding of charged analytes within the Debye length, denoted as λ_D, to attain the probability of direct charge transfer to the material sensing channel. The transfer curve of the GFET device is segmented into two branches at the Dirac point (see Fig. 2b).[53] The left side of the curve illustrates a P-type channel, where holes serve as the charge carriers, while the right side depicts an N-type conduction channel, with electrons acting as the charge carriers.

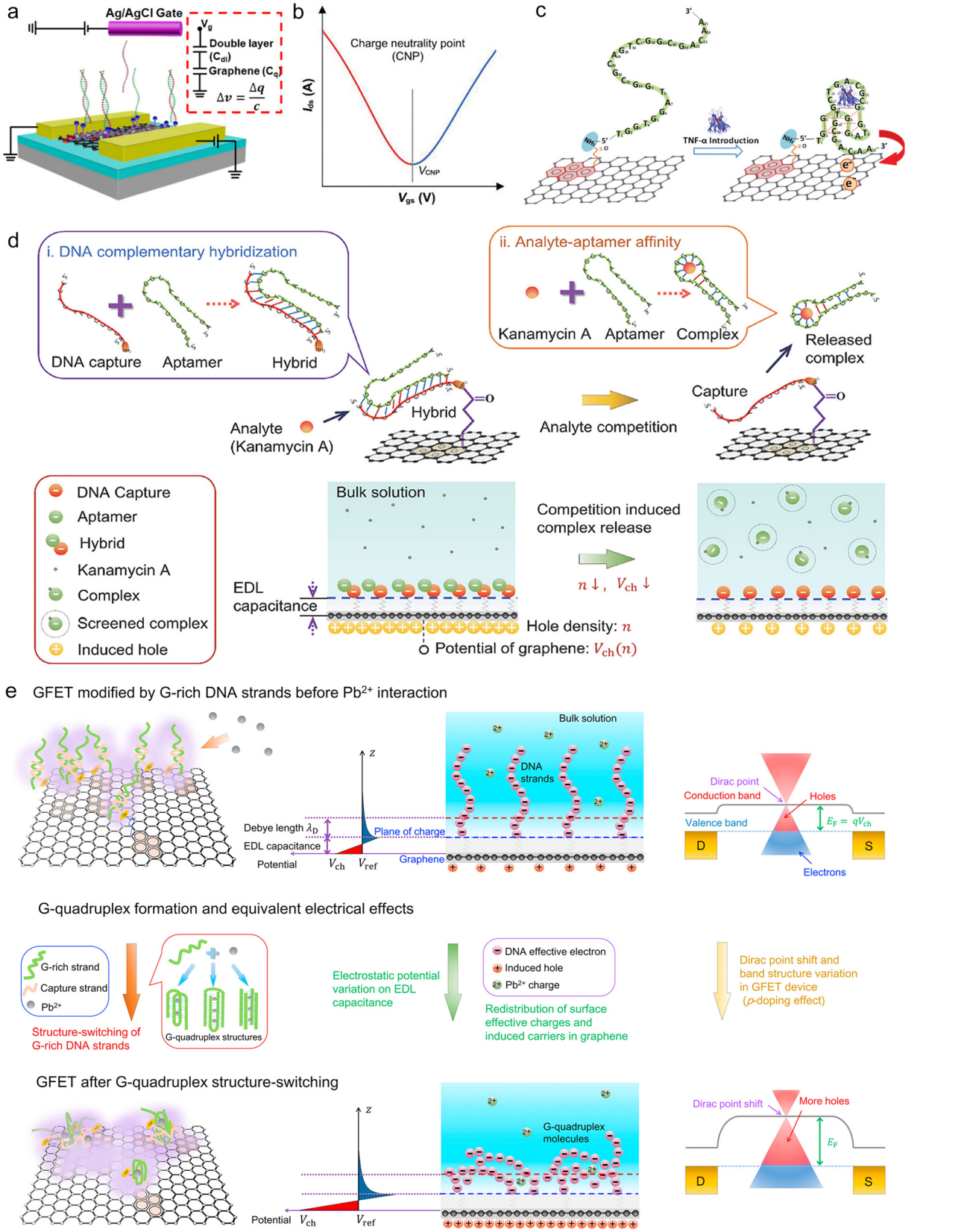

Fig. 2 Working mechanism of GFETs. a) A schematic diagram of a double electric layer capacitor consisting of two parts: interface capacitor and quantum capacitor. Reproduced with permission.[51] Copyright 2022, *Analytical Chemistry*. b) Transfer characteristic curve of graphene. Reproduced with permission.[53] Copyright 2023, *Advanced Functional Materials*. c) The VR11 aptamer folds TNF-α onto the graphene surface, causing a direct transfer of charge. Reproduced with permission.[54] Copyright 2018, *Nanoscale*. d) The sensor for detection of kanamycin A was designed by using the competitive complementary hybridization mechanism of single DNA strands. Reproduced with permission.[55] Copyright 2016, *Advanced Functional Materials*. e) The DNA strand folds into a G-quadruple structure to detect Pb^{2+}. Reproduced with permission.[56] Copyright 2017, *Biosensors and Bioelectronics*.

Farid *et al.* reported a GFET biosensor utilizing a short-length aptamer for IFN-γ detection.[59] As the aptamer's length is short, they proposed that IFN-γ-aptamer binding takes place within the λ_D. Thus, the resulting charge is still not fully screened, resulting in the allocation of electrons to the graphene surface. This process results in an increase in the n-conduction current, which is effectively "sensed" by the graphene. Similarly, Wang *et al.* observed binding interactions between IgE and aptamer molecules even at high salt ionic strengths (450 mM).[60] They hypothesized that after IgE capture, the conformational structure of the aptamer underwent a major change, bringing aromatic nucleotide chains containing a large amount of electrons in contact with the graphene surface. This conformational structure, upon folding, is believed to reach within the λ_D range, enabling a direct transfer of the nucleotide's charge to the graphene surface.

In addition to opting for a shorter aptamer to ensure binding within the Debye length, an alternative strategy involves utilizing a longer aptamer for binding to the tested object. In this approach, the aptamer structure can be folded several times close to the graphene, resulting in N-type doping, where electrons are transferred directly from the biomarker or aptamer to the graphene sensing surface.[54] For instance, in the interaction between insulin and the IGA3 aptamer, a left shift of V_{Dirac} is observed, indicating the doping of more electrons (N-type charge carriers) into graphene.[61] IGA3 aptamers trap insulin and fold, causing charge transfer and bringing electrons to the graphene surface. Fig. 2c provides an explanation for the fact that the original uncoiled G-quadruple aptamer can be transformed into a more rigid parallel or antiparallel curled structure when detecting insulin or TNF-α. The detection mechanism is similar to IgE bound to aptamers.

2.2 Electrostatic induction theory

In addition to the theoretical explanation of N-type doping caused by direct electron transfer, an alternative theory proposing ion adsorption, charging of the EDL capacitance, and electrostatic induction on the graphene surface has garnered substantial support. For instance, Zhu *et al.* devised a solid-gated sensor for pH sensing.[62] It is found that the transconductance of graphene transfer curves is basically the same at different pH levels, suggesting that carrier mobility remained relatively constant despite pH variations. The researchers hypothesized that the primary sensing mechanism involves charge sensing, leading to the charging of the EDL capacitor.

In contrast to previous aptamers that facilitate direct charge transfer on the graphene surface after analyte analysis, electrostatic induction can also be induced on the graphene surface by aptamers adopting hairpin or G-quadruplex structures.[63] Wang and colleagues engineered a sensor for kanamycin A detection using a competitive complementary hybridization mechanism with single strands of DNA (see Fig. 2d).[55] Initially, aptamer molecules are hybridized with complementary short DNA strands, forming a double-stranded DNA hybridization structure affixed to the graphene. Upon addition of kanamycin A, the aptamer binds to the analyte molecules, forming hairpin complexes and detaching from the graphene surface. Prior to the competitive binding separation of the analyte, the hybrid molecules, which are negatively charged, induce electrostatic effects on the EDL capacitor at the solution interface, thereby increasing the concentration of hole carriers in the graphene. During the competition process, the negatively charged hairpin complex is released into the solution and is shielded after dissociating from the λ_D. As a result, the occurrence of N-type doping leads to the decrease of the hole density of graphene.

Li *et al.* used a G-quadruple-structure switch to detect Pb^{2+}.[56] In their GFET sensor, when Pb^{2+} is present, the DNA strand folds to encapsulate Pb^{2+} ions within a G-quadruplex structure (refer to Fig. 2e). Subsequently, a greater portion of the DNA's charge migrates towards the charged surface of the EDL, inducing holes in the graphene electrostatically through the equivalent capacitance of the EDL. This mechanism augments the population of hole carriers, facilitating P-type doping of the graphene sensor, thereby enabling low-label biosensing of Pb^{2+}.

In addition to the self-folding of DNA strands influencing charge sensing, the proximity of biomolecules to the graphene surface induced by DNA strands can also modify the graphene carrier concentration. For instance, Hao *et al.* devised a GFET for detecting interleukin-6 (IL-6).[64] After binding to IL-6, the aptamer folds near the graphene sensing channel. IL-6 comprises negatively charged aromatic amino acids, inducing equivalent hole carriers at the graphene interface through electrostatic induction, which subsequently charges and discharges the capacitors at the graphene–solution interface.

3. GFETs with different gate configurations

The architecture of most GFET biosensors primarily consists of three components: the sensing channel made of two-dimensional sensitive materials, the drain/source, and the gate.[65,66] Consequently, the classification of GFETs is based on the structural layout of the gates, which are divided into several types: external Ag/AgCl gate, planar gate, back gate, top gate, and floating gate. For GFET biosensors to detect biomarker concentrations, they must first be modified with a probe that can bind to the target biomarker. The binding process between the probe and the target causes a change in the charge of the EDL capacitance, changing the carrier concentration within the 2D material, facilitating the transduction of biological signals. Depending on the location of the probe modification, the mechanisms that cause the change of carrier concentration in two-dimensional materials can be roughly divided into the following situations: (1) the

probe is modified on the surface of the 2D material,[39] where the interaction between the probe and the biomarker directly alters the charge carrier concentration within the 2D material. (2) The probe is modified on the gate surface, where the binding of the probe and biomarker occurs.[67] The shape of the probe or the charge distribution in the gate area is changed, which indirectly causes the change of the carrier concentration inside the 2D material.

3.1 External Ag/AgCl gate

The external Ag/AgCl gate is directly inserted into the detection solution, and by the coupling effect of the EDL capacitance, the charge carrier concentration in the 2D material could be effectively adjusted. The external Ag/AgCl gate configuration is widely employed in GFET structural design (see Fig. 3a), particularly in biomarker detection. The graphene channel as the sensing part of the GFET sensor, using a new graphene transfer method,[68] or adjusting the traditional flat channel to a pleated channel changes the sensing performance of the GFET, such as the sensing response time and sensitivity. In addition, the sensor recognition unit, as an important part of the GFET sensor, can improve the sensitivity and reliability of the sensor by introducing structural improvements or special aptamer types.[69] The sensor illustrated in Fig. 3b is customized with antibodies targeting the SARS-CoV-2 spike protein on the GFET. The minimum detection concentration in the clinical transport medium for this sensor is 100 fg mL^{-1}.[26]

Li *et al.* introduced an MXene-GFET sensor using a polymer connecting MXene and graphene.[74] The sensor was evaluated using a recombinant 2019-nCoV spike protein antigen at concentrations ranging from 1 to 10 pg per milliliter. The response time of the MXene-GFET platform was approximately 50 ms, with an impressive LOD for the recombinant spike protein of 1 fg mL^{-1}, underscoring the sensitivity of the platform for virus detection. Similarly, Kang and colleagues adapted the S1 protein to a GFET, achieving an LOD of about 150 antibodies per 100 μL of whole serum and reducing the diagnostic time for testing clinical serum samples to a mere 2 minutes.[75]

In addition, Kong *et al.* reported the method of using a Y-shaped double probe to simultaneously capture two genes in COVID-19 nucleic acid.[70] The structure of the Y-dual probe allows it to detect not only the ORF1ab gene but also the N gene (see Fig. 3c). It has a high recognition rate in the detection process of 1 min and realizes the breakthrough achievement of direct five-in-one hybrid detection for the first time.

In order to reduce the steps of virus purification and achieve rapid sample detection, Park *et al.* used RT-LAMP technology to rapidly achieve RNA amplification.[71] The consumption of RT-LAMP primers was detected using a crumpled graphene FET. Among them, the negative samples will cause the detection curve to shift beyond the monitoring threshold, while the positive samples have the opposite effect, realizing the discrimination of COVID-19 patient samples (Fig. 3d).

Wang *et al.* developed a molecular-scale detection system that uses bovine serum albumin as an antifouling layer to facilitate rapid detection of nucleic acids in whole serum.[68] The system consists of a self-assembled rigid tetrahedral DNA structure adsorbed on graphene as a base, and is then modified by a single-stranded DNA cantilever and aptamer probe (see Fig. 3e). The MolEMS GFET can detect COVID-19 nucleic acid at a concentration of 0.02 copies per μL and can determine whether a nasopharyngeal swab sample is positive within 4 minutes.

Hwang *et al.* employed a crumpled GFET electrical biosensor to detect miRNA let-7b sequences in human serum (refer to Fig. 3f).[72] Compared to flat graphene, the crumpled GFET biosensor exhibits an exceptionally low LOD of only 600 zM. The researchers hypothesized that the nanoscale bending and deformation of crumpled graphene could increase the λ_D between the sensing channel surfaces and electrolytes, thus significantly enhancing the sensitivity of crumpled GFET sensors.

Rodrigues *et al.* investigated the stability and charge distribution of peptide nucleic acids (PNAs) and applied them to GFET sensors as aptamers. To compare the performance of PNA and DNA aptamers, they were utilized together to detect cardiac troponin I (cTnI) protein.[76] Furthermore, they found that PNA and DNA aptamers exhibit similar dissociation constants and detection limits in PBS, and PNAs can also adapt to complex biological fluids.

Fig. 3g illustrates graphene field-effect transistors (GFETs) employing carbon dots (CDs) to cover the sensing region of graphene.[73] The LOD of exosomes detected by the CD-GFET sensor can be reduced to 100 particles per μL. This suggests that the modification of the graphene surface with carbon dots effectively enhances the capture speed and sensitivity of the sensor for exosomes.

Weng *et al.* introduced an approach to nucleic acid detection utilizing CRISPR and Cas technology, presenting the CRISPR Cas12a-mediated GFET, termed CRISPR Cas12a-gFET.[49] The sensor was employed to detect synthetic target genes of human papillomavirus and *Escherichia coli* plasmids, respectively, with detection limits of 1 aM and 10 aM (see Fig. 3h). The advantage of the Cas12a-gFET sensor over the Cas9 sensor[77,78] lies in its ability to detect ssDNA in addition to dsDNA.

Fig. 3i depicts a sensor modified with a synthetic nucleotide aptamer.[47] This modification of the traditional aptamer sensor enables the AN-Apta-FET to specifically detect liver cancer exosomes with a LOD of 242 particles per mL, addressing the limitation of traditional aptamer sensors in distinguishing between various tumor-derived exosomes. The synthetic synthesis of the aptamer repertoire has expanded the range of biomarkers detectable by GFET biosensors.

3.2 Planar gate

Conventional electrolytically gated GFETs necessitate an additional gate outside the drain–source electrode plane,

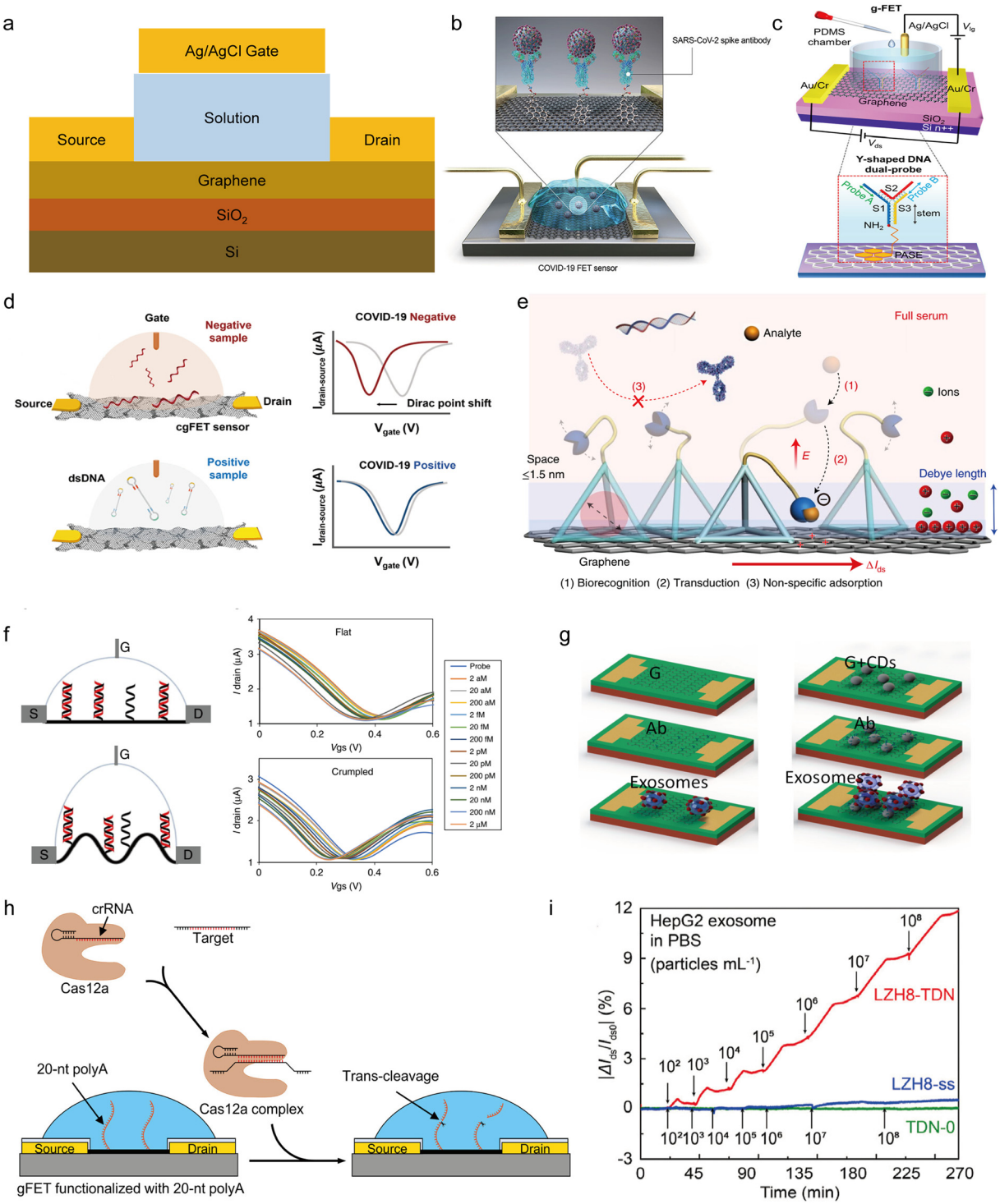

Fig. 3 External Ag/AgCl gate configuration of the GFET. a) External Ag/AgCl gate in the solution gate configuration. b) A typical external Ag/AgCl gate configuration in the GFET structural design. Reproduced with permission.[26] Copyright 2020, *ACS Nano*. c) The Y-shaped probe enables simultaneous detection of multiple genes. Reproduced with permission.[70] Copyright 2021, *Journal of the American Chemical Society*. d) Crumpled graphene FETs (cgFETs). Reproduced with permission.[71] Copyright 2021, *ACS Sensors*. e) MolEMS consisting of a ssDNA cantilever and self-assembled tetrahedral double-stranded dsDNA. Reproduced with permission.[39] Copyright 2022, *Nature Biomedical Engineering*. f) Crumpled GFET biosensor to detect miRNA. Reproduced with permission.[72] Copyright 2020, *Nature Communications*. g) Carbon dot (CD) modified graphene for exosome detection. Reproduced with permission.[73] Copyright 2021, *ACS Applied Materials & Interfaces*. h) Schematic diagram of the CRISPR Cas12a-gFET trans-cutting 20-nt polyA probe. Reproduced with permission.[49] Copyright 2023, *ACS Sensors*. i) Three artificial nucleotide aptamers were used for the specific detection of hepatoma exosomes. Reproduced with permission.[47] Copyright 2023, *Analytical Chemistry*.

significantly impacting the miniaturization of the device. Under the working conditions of external Ag/AgCl electrodes, the EDL capacitance at the solution–graphene interface functions as a gate medium. The insertion of these electrodes may induce fluctuations in the electrical properties of 2D materials.[79] However, by integrating three electrodes – namely, the gate and drain–source electrodes – on the same flat surface (refer to Fig. 4a and b),[28,45] thereby eliminating the requirement for external gates,[80] such planar gate FETs have also found widespread application in graphene Hall elements,[27] pressure sensors,[81] and biomarker detection.[67,82]

Kim *et al.* successfully fabricated ion-gated graphene Hall element (ig-GHE) arrays.[27] ig-GHE devices typically operate with an ion V_g of 0.35 V, a V_{gs} of 0.2 V, and a drain current below 1 μA. At these parameters, the ig-GHE device achieves a minimum magnetic resolution of approximately 0.3 G Hz^{-1}. The high sensitivity of the ig-GHE device to magnetic fields at low voltages is attributed to the excellent carrier tunability in ion gating.

Fig. 4c illustrates a pressure sensor utilizing β-glycine/chitosan as an insulator to form a metal–insulator–metal (MIM) sandwich structure.[81] Due to the sensitive layer of the three-layer sandwich structure, the sensor can operate at an operating voltage of 50 mV. In addition, the sensor exhibits variable sensitivity in the pressure range from 5 to 20 kPa and from 20 to 35 kPa.

Deng *et al.* fabricated carbon quantum dot (CQD) modified GFETs for label-free DNA detection.[85] CQDs were modified on the gate using thioglycolic acid, and then the ssDNA probe was adsorbed to the CQDs by π–π adsorption (refer to Fig. 4d). The sensor demonstrates a detection range for DNA from 1 aM to 0.1 mM.

Similarly, Zhang *et al.* synthesized boric acid groups to CQDs and modified CQDs to the gate of a planar gate GFET sensor.[86] By detecting sialic acid, the planar gate sensor exhibited a detection range from aM to μM, with a sensitivity reaching 10^{-19} M.

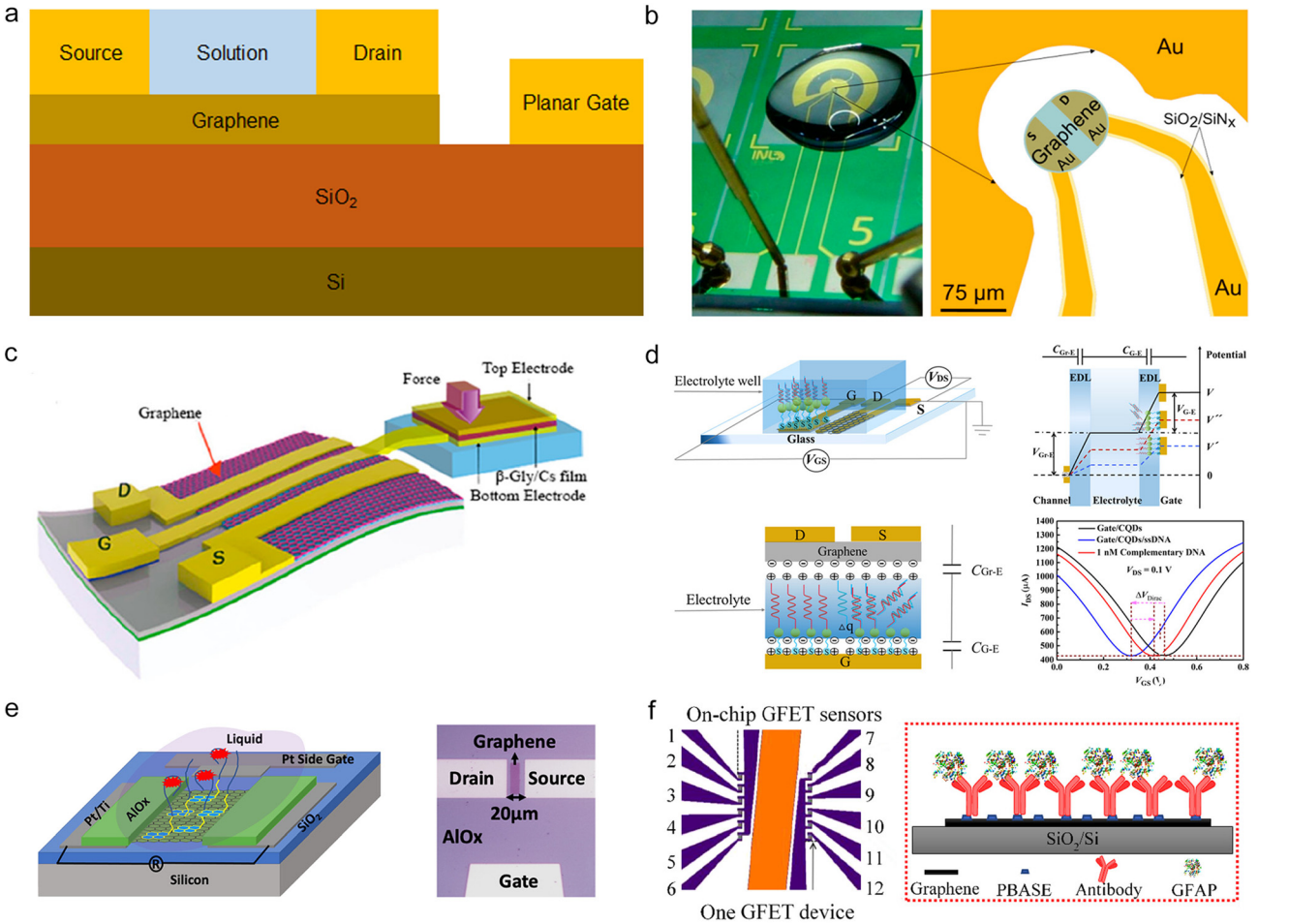

Fig. 4 Planar gate configuration of GFETs. a) Diagram of a planar gate in a solution gate configuration. b) Optical image of a planar transistor chip, including the source (S), drain (D), and gate (local view). Reproduced with permission.[45] Copyright 2019, *ACS Sensors*. c) The pressure sensor uses a β-Gly/Cs film as the sensitive layer. Reproduced with permission.[81] Copyright 2020, *ACS Applied Materials & Interfaces*. d) Planar gate GFET using carbon quantum dots (CQDs). Reproduced with permission.[67] Copyright 2022, *Analytical Chemistry*. e) GFET sensor with planar side-gate Pt electrodes. Reproduced with permission.[83] Copyright 2022, *ACS Nano*. f) Planar GFET array with a common gate. Reproduced with permission.[84] Copyright 2022, *ACS Sensors*.

Fig. 4e depicts a GFET sensing device for the detection of multiple opioid metabolites.[83] Kumar and colleagues designed a planar gate sensor with integrated side (Pt) electrodes. The detection limits for noroxycodone (NX), 2-ethyl-1,5-dimethyl-3,3-diphenylpyrrolidine (EDDP), and norfentanyl (NF) were 38, 27, and 42 pg mL^{-1}, respectively, in wastewater diluted 20-fold with buffer.

Xu *et al.* conducted research on the detection of glial fibrillary acidic protein (GFAP), a type of biomarker associated with various neurological diseases and utilized for detecting traumatic brain damage (refer to Fig. 4f).[84] The sensor they developed achieved a LOD of 400 aM in PBS and 4 fM in human plasma. Compared with ELISA, the GFAP GFET demonstrated the ability to significantly reduce the detection time of patient samples and enhance detection sensitivity.

3.3 Back gated configuration

In addition to the traditional liquid gate GFETs, GFET sensors with back gated or buried gated configurations (refer to Fig. 5a) are also widely used for detection of nucleic acids,[87] exosomes, biological small molecules,[88] *etc.* The external Ag/AgCl gate and planar gate generate a gating electric field that penetrates the sample solution, and this gating electric field may interfere with the affinity binding between the biomarker and the probe, thus reducing the stability of the biosensor.[89] The back gating configuration is placed through the back of the gate to isolate the gate from the solution. In the structural design of back gates, SiO_2 is predominantly used as the dielectric layer. Due to the low dielectric constant of SiO_2 (ε = 3.9), a working gate voltage (V_g) of 40–50 V is required, posing potential risks to the human body. It is necessary to utilize oxide layer materials with higher dielectric constants to ensure greater safety.

Huang and colleagues implemented a back gate to achieve gated doping and used a dielectric layer of Al_2O_3 to reduce the gate voltage, thereby enhancing the detection performance for miRNA.[90] They developed a dual-gate GFET incorporating a graphene oxide/graphene (GO/G) layered structure for the detection of miRNA-21 (refer to Fig. 5b).

The sensitivity of the sensor using only a single V_g is 19.26 mV dec^{-1}, and when the back gate is utilized for gating doping in dual-gate control, the sensitivity of the sensor increases to 33.65 mV dec^{-1}. The sensor exhibits a linear response to miRNA concentrations ranging from 10 fM to 100 pM.

Kordrostami *et al.* depicted a flexible back-gated sensor designed for glucose detection.[92] This sensor consists of a back-gated GFET fabricated by stacking CuO hollow spheres on a flexible PET substrate. Glucose concentration detection is performed in two modes: resistance and FET. The results indicate that the FET mode yields a greater current compared to the resistance sensor. In this work, the sensitivity of the flexible sensor for glucose detection is reported to be 600 aM, with a LOD of 1 nM.

Gao *et al.* developed a back-gated configuration GFET modified with a hairpin DNA probe.[29] This sensor enables signal amplification for nucleic acid detection through hybridization chain reaction (refer to Fig. 5c). The detection limit for 21-mer was approximately 5 fM, albeit with a longer detection time of 1 hour. The same research group also created an aptamer sensor for arsenate detection using a

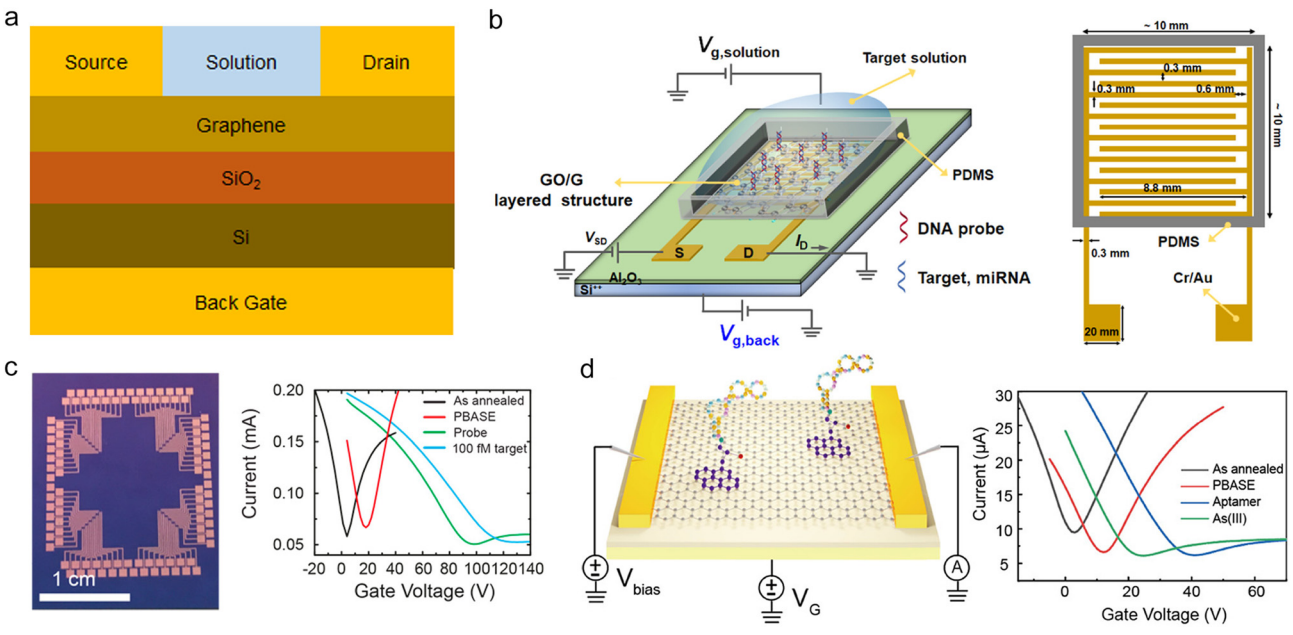

Fig. 5 Back gated configuration of GFETs. a) Diagram of a back gated configuration of a GFET. b) Dual gate GFET with planar interfinger electrodes. Reproduced with permission.[90] Copyright 2021, *ACS Applied Electronic Materials*. c) A back gated configuration GFET sensor for nucleic acid detection based on hairpin probe DNA. Reproduced with permission.[29]Copyright 2018, *Nano Letters*. d) Back gated GFET for arsenate detection. Reproduced with permission.[91] Copyright 2022, *ACS Applied Nano Materials*.

similar reverse-gating configuration.[91] Furthermore, the aptamer folds upon binding with arsenate, introducing negative charge to the surface of the sensing channel, enabling the detection of arsenate in the range of 0.05 to 1000 ppb (refer to Fig. 5d).

Klein *et al.* developed back-gated GFETs for the selective detection of exosomes.[93] In this device, a microfluidic channel exposes a graphene film conjugated with an anti-CD63 antibody to the solution. However, this sensor is currently limited to sensing a low concentration of exosomes at 0.1 μg mL^{-1}, and further studies are needed to enhance the efficiency of antibodies in trapping exosomes.

3.4 Top gated configuration

Due to the advantages of top-gated structure FETs (refer to Fig. 6a), such as the obvious gate gating effect and effective reduction of parasitic capacitance, their research direction is mainly focused on frequency doublers,[94] radio frequency applications,[95,96] biological detection using nanogaps inside the top gate,[97,98] *etc.*

Jung *et al.* assembled a top gated GFET with Al_2O_3 as a dielectric layer.[101] They fabricated the Al_2O_3 dielectric layer by atomic layer deposition (ALD) and PMMA wet transfer, and further compared the hole mobility of the GFET with the two processing methods. It was found that PMMA wet transfer could reduce the damage to the graphene membrane and avoid the doping of graphene produced by ALD.

The electron mobility of two-dimensional materials can be affected by the insulating substrate. Kim *et al.* reported the growth of a silicon nitride (SiON) single crystal insulating layer on SiC wafers.[99] They fabricated two types of top-gated GFETs with SiON/SiC wafers and SiO_2/Si wafer substrates (see Fig. 6b). In a comparison experiment between the SiON/SiC wafer and SiO_2/Si wafer, the graphene electron mobility can be increased by about 1.5 times using SiON/SiC wafers.

In addition, when the top and back gates are combined to form a double gate structure, the transconductance of the GFET can be improved. Hwang *et al.* conducted measurements and comparisons of the transfer characteristic curves of dual-gate GFETs and single-top gated GFETs.[102] The maximum transconductance of the DG-GFET can be up to 1.5 times that of the SG-GFET, demonstrating the potential of the multi-gate architecture for improving GFET performance.

Fig. 6c illustrates a pressure sensor based on back gate and movable top gate design GFETs.[31] Performance analysis indicates that the movable top gate can potentially detect nanoscale displacements, and the structural design of the double top gate can also provide higher sensitivity than the single top gate.

Kumada *et al.* fabricated a graphene photodetector with a ZnO top gate.[100] The single layer of graphene in the photoelectric conversion region is encapsulated by double layer hBN (Fig. 6d). By measuring the temporal distribution of the photocurrent in the sample, Kumada *et al.* provided a new explanation for the O–E transition mechanism in graphene, with the help of the time-controlled phenomenon of photocurrent generation.

The biodetection applications utilizing the top gate configuration involve the creation of a nanogap within the top gate oxide. When the target substance and the bioprobe interact within this nanogap, it alters the effective gate capacitance, resulting in signal transduction.[98] Amiri *et al.*

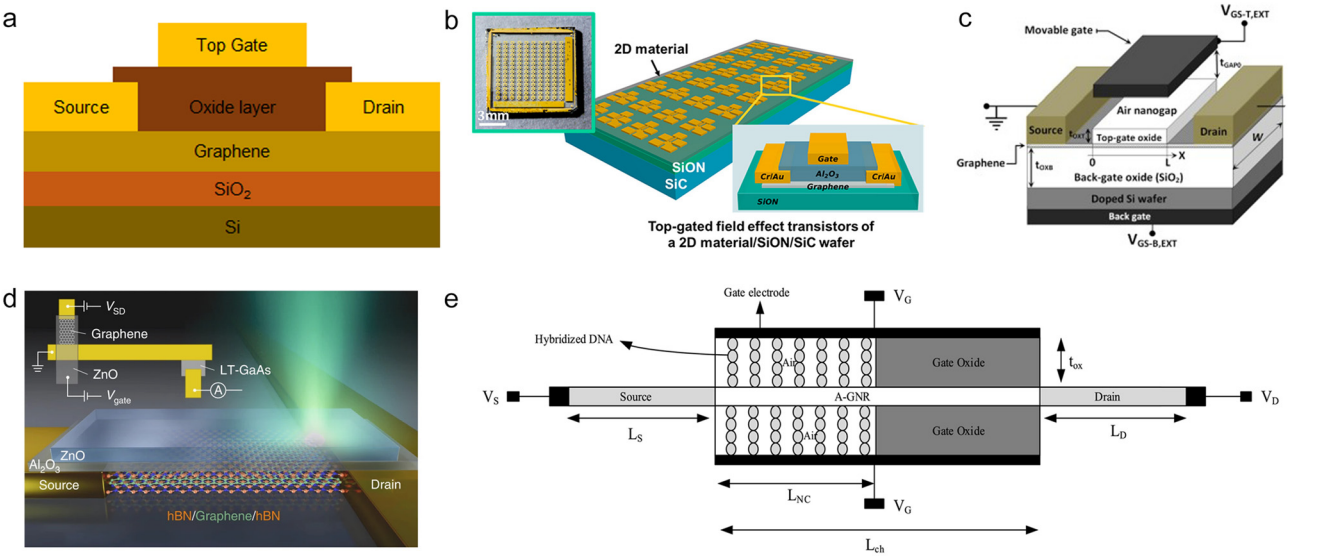

Fig. 6 Top gated configuration of GFETs. a) Diagram of a top gate configuration of a GFET. b) Top-gated FET of a 2D material/SiON/SiC wafer. Reproduced with permission.[99] Copyright 2023, *Nano Letters*. c) A dual-gate pressure sensor with a movable top gate. Reproduced with permission.[31] Copyright 2020, *AEU - International Journal of Electronics and Communications*. d) A graphene photodetector using ZnO as a top gate. Reproduced with permission.[100] Copyright 2022, *Nature Photonics*. e) DNA hybridization detection is implemented in the nanogap at the top gate.[97] Reproduced with permission. Copyright 2020, *Materials Science and Engineering: C*.

constructed nanogaps inside gate oxides and modified targeted DNA to detect the DNA of *Neisseria gonorrhoeae* (Fig. 6e). With a biosensing detection area of only 240 nm^2, they achieved a relative sensitivity of about 1 mV nm^{-2}, potentially yielding a highly sensitive and compact biosensor.[97]

3.5 Floating gated configuration

The floating gated structure can capture and release electrons, thereby changing the charge carrier density of the active dielectric layer, so the GFET of the floating gated structure (Fig. 7a) can be used in logic operations,[103] data storage,[104–106] rectifier switching,[107] *etc.*

Fig. 7b shows a logic device based on a three-layer heterogeneous structure; the three-layer material distribution is WSe_2/h-BN/graphene.[108] Through the change of operating voltage such as the drain and the floating gate, the bipolar WSe_2 can realize switchable AND and XNOR logic operations, ensuring the reconfigurable logic operation ability of the device.

Traditionally, biomarker detection relies on a solution environment as a carrier. However, Wang *et al.* proposed a fully-solid-state (FSS) transistor.[112] In this approach, graphene is already encapsulated in a solid dielectric material. To create a biomolecular interaction-sensitive interface, Wang *et al.* introduced a functionalized metal floating gate to the top layer of the dielectric. The solid dielectric layer above the graphene enhances its gating efficiency compared to the traditional solution EDL interface. As a result, the sensor achieved a concentration LOD of 929.8 fM using a Pb^{2+} unlabeled DNA enzymatic bioassay.

Sheibani *et al.* designed a sensor based on a platinum expansion gate.[109] The separation of the sensing region and electrical energy conversion is achieved by transferring graphene to the gate of platinum. In a physiological fluid environment, the device can detect cortisol concentrations in the λ_D range with a LOD of 0.2 nM from 1 nM to 10 μM. They also proposed a 3D sensing concept (see Fig. 7c).

Fig. 7d depicts a remote floating gated (RFG) FET.[110] The sensor was primarily utilized for detecting the SARS-CoV-2 S protein, with a sensitivity of 5.1 mV dec^{-1} in saliva mixed solutions. The floating gate structure electrically isolates the sensing material through an insulator and connects it with the gate capacitance of the FET transducer to achieve signal transmission. No current flows through the sensing material area, thereby preventing adverse effects of interface traps, defects, and redox reactions of the sensing material itself. Recently, this research group reported the application of a RFGFET for diagnosing nasopharyngeal swab samples (Fig. 7e).[111] In this study, the sensor was capable of directly detecting nasopharyngeal swab samples collected from patients, achieving an accuracy of label-free SARS-CoV-2 detection of 90.6%, with high repeatability.

To date, the development of GFET biosensors based on various gate configuration strategies has achieved relatively abundant progress. Table 1 summarizes the potential application scenarios and advantages of various gate configurations and provides a comparative overview of their sensing performance across specific applications.

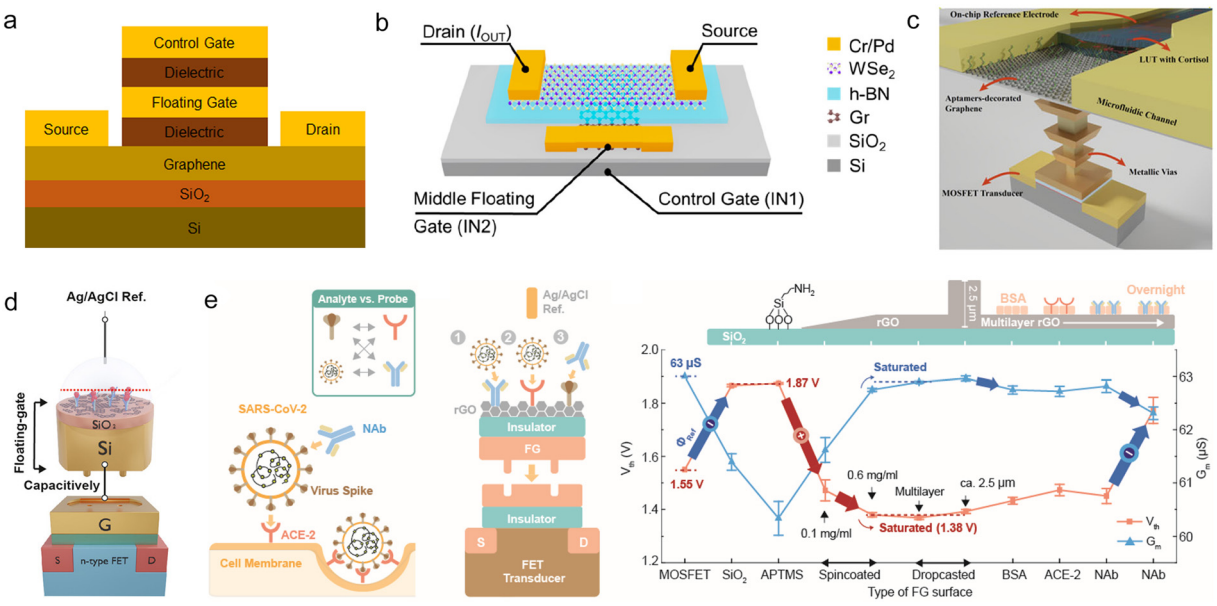

Fig. 7 Floating gated configurations of GFETs. a) Diagram of a floating gate configuration of a GFET. b) MFGFET device with a three-layer heterogeneous structure for logic operation. Reproduced with permission.[108] Copyright 2023, *Nano Letters*. c) A concept of an integrated cortisol sensor using a back gate configuration. Reproduced with permission.[109] Copyright 2021, *Communications Materials*. d) A remote floating-gate (RFG) FET. Reproduced with permission.[110] Copyright 2022, *ACS Applied Materials & Interfaces*. e) Schematic representation of a RFGFET modifying NAb or ACE-2 probes. Reproduced with permission.[111] Copyright 2023, *ACS Applied Materials & Interfaces*.

Table 1 Performance summary of GFET biosensors with different gate configurations

Gate configurations	Advantages	Target	Material	Probe position (signal transduction)	LOD	Response time	Ref.
External Ag/AgCl gate	Effectively modulates the charge carrier concentration, convenient operation process	ssDNA	Crumpled graphene	Sensitive material surface	—	35 min	71
		SARS-CoV-2 nucleic acid	Graphene	Sensitive material surface	0.02 copies per μL	0.1–4 min	39
Planar gate	Avoids electrical disturbance caused by external electrode insertion, high integration, compact component structure, suitable for flexible wearable applications	ssDNA	Graphene	Gate surface	1 aM	5.4 min	67
		Glial fibrillary acidic protein	Graphene	Sensitive material surface	4 fM	<15 min	84
Back gate	Avoids the interference of the liquid gate gating on the combination of the target and biological probe, compact component structure. The high dielectric constant oxide layer can reduce the gate voltage, suitable for portable applications	miRNA-21	Graphene oxide/graphene	Sensitive material surface	10 fM	—	90
		Arsenite	Graphene	Sensitive material surface	0.02 ppb	1 s	91
Top gate	The sensing area exhibits high sensitivity per unit area and a compact overall layout	DNA	Graphene	Sensitive material surface	—	—	97
Floating gate	Avoids the adverse effects of interface traps, defects, and redox reactions of the sensing material itself, high reliability and less time drift	SARS-CoV-2 S protein	rGO	Sensitive material surface	—	5 min	110
		SARS-CoV-2 spike protein	rGO	Sensitive material surface	5×10^{-2} TU ml^{-1}	<5 min	111

4. GFET array toward multiplex detection

Arrays and multiplexing of sensors are highly appealing for the simultaneous detection of viruses, nucleic acids, and antigen proteins.[113,114] Multiplex sensing methods can be categorized into two main approaches: (1) simultaneous detection of multiple markers: this approach involves measuring a variety of markers concurrently. Multiple sensing units are combined to independently detect various markers, generating separate detection signals for integrated analysis.[38,115] (2) Detection of the same marker in multiple modes or devices: in this approach, the same marker is detected using multiple modes or devices.[116–120] The reliability of the measurement process is ensured by cross-validating multiple sets of data.[121]

In the production and application process of GFETs, how to achieve reuse and cost saving is always faced with problems. Dai *et al.* achieved a modular design in which the GFET is reversibly assembled and disassembled by splitting the sensor into independent biometric and sensing modules (Fig. 8a).[44] Among them, the biometric module is mainly PEG hydrogel, and penicillinase or urease is added as a recognition probe to detect penicillin G and urea.

Fakih *et al.* developed a multi-ion sensitive FET array,[122] which can simultaneously measure K^+, Na^+, NH_4^+ and other ions, and also monitor the changes in ion concentration caused by mineral absorption by detecting the growth of aquarium plants (Fig. 8b).

There are many kinds of biomarkers for Alzheimer's disease, such as Aβ1–42 and t-Tau. Fig. 8c illustrates the differentiation and multiple detection achieved by exploiting differences between biomarker isoelectric point values. The LOD of fM concentration can be reached in biological fluids including human plasma and artificial cerebrospinal fluid.[123]

Lyme disease, primarily caused by *Borrelia burgdorferi*, can result in stiff and swollen joints as well as damage to the cardiovascular system. Gao *et al.* designed a four-quadrant GFET for the simultaneous detection of multiple Lyme disease antigens.[127] This method utilizes four antibodies to modify four quadrants, enabling simultaneous detection in four lanes at concentrations as low as 2 pg ml^{-1}.

Sweat is an important body fluid, rich in chemicals that reflect the metabolic and physiological states of the human body. Wearable sweat analysis enables non-invasive and continuous biomarker monitoring. Wang *et al.* fabricated graphene electrodes on a polyimide (PI) substrate and combined several modules, such as microfluidic components, to create a flexible sensor patch.[124] The patch could induce and collect sweat, and further detect the concentration changes of leucine, tryptophan, and other amino acids in sweat (see Fig. 8d). The researchers further demonstrated wearable and continuous monitoring of amino acid changes after meals.

The multiplexing of GFETs has also been developed in terms of recording the electrical activity of neurons and constructing sensing neural interfaces. Because of its good biocompatibility, graphene can be developed as a neural probe to detect the potential of the cerebral cortex. Fig. 8e showcases a flexible sensing system comprising a 64-channel g-SGFET array.[43] This system demonstrates the stability and excellent biocompatibility of the graphene array neural probe. The probe's performance was evaluated by monitoring a freely moving rat model continuously for 24 hours over an extended period.

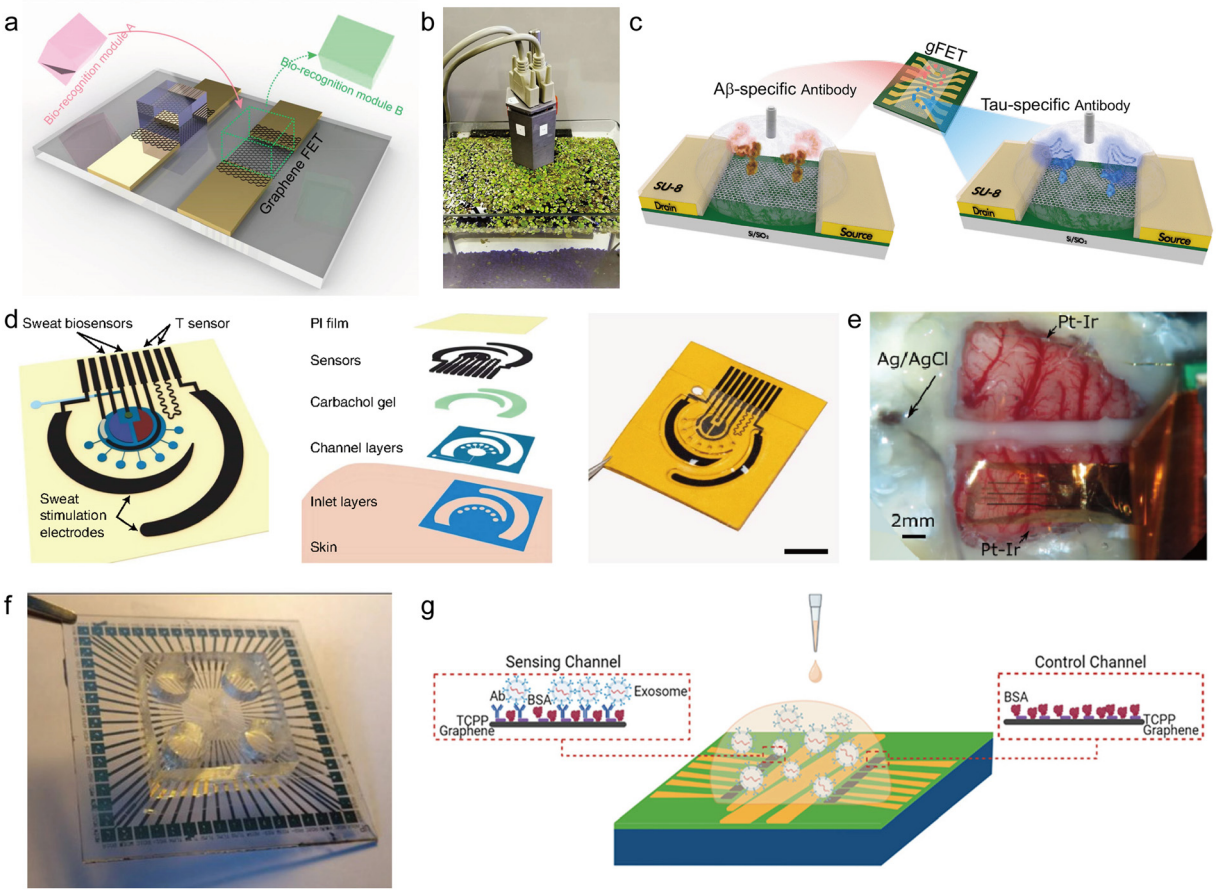

Fig. 8 GFET array toward multiplex detection. a) The GFET sensor that can replace the biometric module. Reproduced with permission.[44] Copyright 2019, *Nano Letters*. b) Detection of change of ion concentration during plant growth. Reproduced with permission.[122] Copyright 2020, *Nature Communications*. c) A multiplex sensor modified with Aβ1–42 and t-Tau antibodies. Reproduced with permission.[123] Copyright 2020, *Biosensors and Bioelectronics*. d) Multiplexed sensor array for the detection of metabolites in sweat. Reproduced with permission.[124] Copyright 2022, *Nature Biomedical Engineering*. e) A neural interface with 64 channels. Reproduced with permission.[43] Copyright 2021, *Nature Communications*. f) GFET array and microfluidic circuit fabricated on a sapphire substrate. Reproduced with permission.[125] Copyright 2022, *Advanced Functional Materials*. g) GFET array for cancer exosome detection. Reproduced with permission.[126] Copyright 2023, *ACS Nano*.

Dupuit *et al.* combined a multi-channel microfluidic platform and a GFETs array for the detection of neurite and nerve spike.[125] The device (Fig. 8f) can detect spontaneous activity in neurons at an early stage of culture, providing multimodal detection of the nerve spike shape and amplitude.

Yin *et al.* integrated multiple sensor arrays on a common gate to detect pancreatic cancer exosomes.[126] This biosensor can accurately distinguish between stage 1 and stage 2 cancer within 45 minutes by detecting specific exosomes expressing GPC-1 (see Fig. 8g).

5. Flexible GFETs toward wearable applications

With the improvement of living standards, people have put forward the demand for early prevention and diagnosis of diseases.[32] Traditional GFETs are mainly rigid substrates, which are not conducive to long-term wear and use of patients.[33,128,129] Flexible sensors are expected to become an important part of wearable devices by virtue of their excellent elasticity and stretchability, small size and easy to carry features.[130] In general, materials used as substrates for flexible GFETs include polydimethylsiloxane (PDMS), polyethylene naphthalate (PEN),[131] Mylar,[132] polyimide (PI),[133] polyethylene terephthalate (PET),[134–136] *etc.*

Initially, flexible GFET sensors mainly use flexible materials instead of silicon substrates[137] and explore the change trend of sensing performance of GFETs after bending, folding and other deformation. Wang *et al.* developed a GFET sensor on a Mylar film.[132] Electrodes were fabricated on a 2.5 μm thick flexible substrate. The sensor was capable of detecting TNF-α under surface deformation with a LOD of 5×10^{-12} M (refer to Fig. 9a). Further, by coating Tween 80 to inhibit non-specific adsorption during TNF-α detection and by pre-stretching to maintain a consistent fit during finger movement (Fig. 9b), the detection limit was reduced to 2.75 pM in artificial tears.[138]

Since the surface of human skin is not uniform, such as human fingerprints, thinner flexible substrates will be more

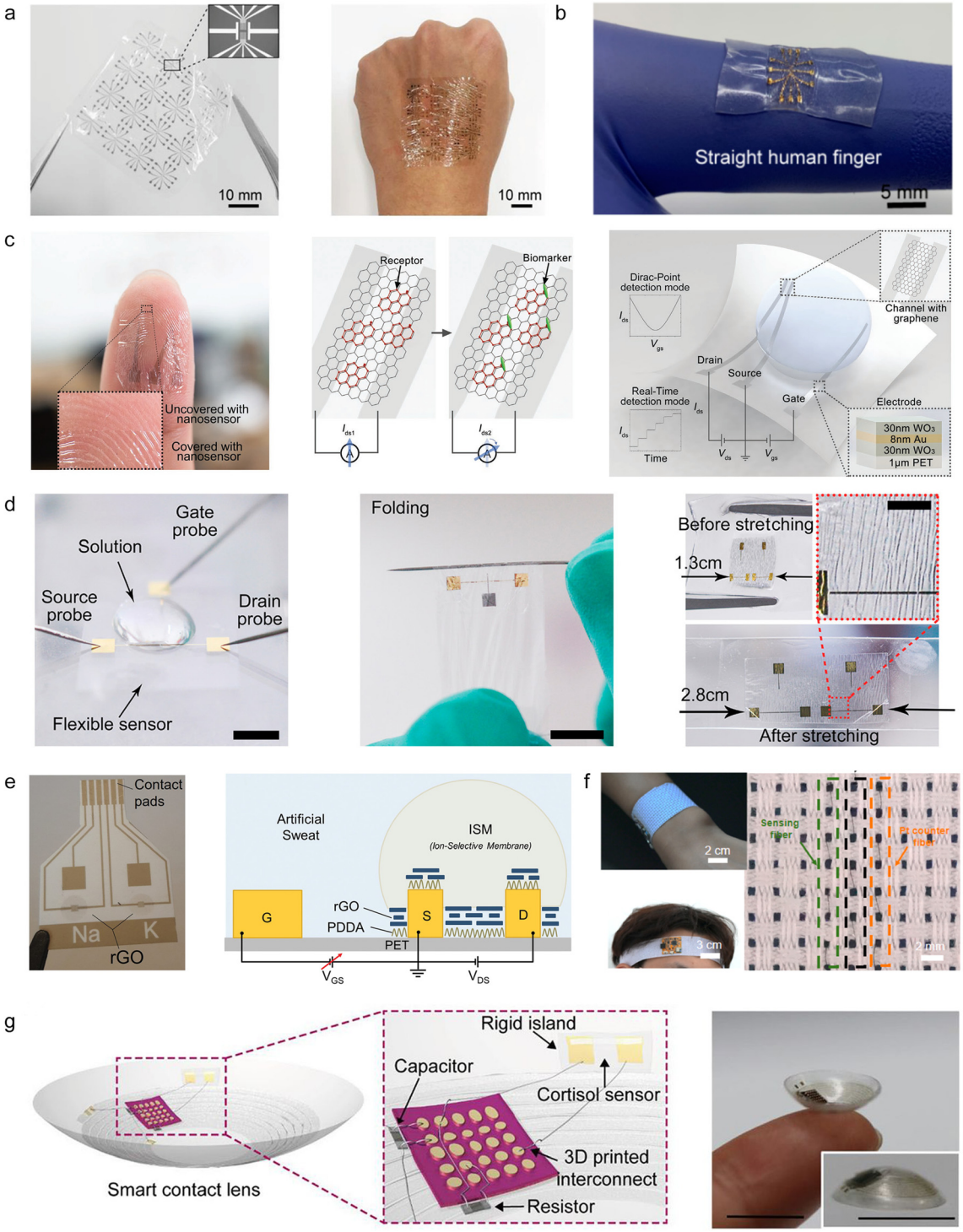

Fig. 9 Flexible GFETs toward wearable applications. a) Flexible GFET prepared on a Mylar film substrate. Reproduced with permission.[132] Copyright 2019, *Advanced Functional Materials*. b) Stretchable biosensors attached to a finger. Reproduced with permission.[138] Copyright 2020, *Nanomaterials*. c) A transparent GFET fabricated on a 1 μm polymer substrate. Reproduced with permission.[46] Copyright 2022, *Advanced Materials Technologies*. d) Stretchable and foldable sensor using a PET substrate. Reproduced with permission.[139] Copyright 2022, *ACS Applied Bio Materials*. e) A sensor for ion detection combined with an ion selective membrane on a PET substrate. Reproduced with permission.[33] Copyright 2022, *Small*. f) Illustration of a headband and wristband woven from carbon nanotube/graphene (CNT/G) composite fibers. Reproduced with permission.[48] Copyright 2023, *Biosensors and Bioelectronics*. g) An integrated wearable contact lens for cortisol detection. Reproduced with permission.[37] Copyright 2020, *Science Advances*.

suitable for the skin. Huang *et al.* proposed a GFET sensor made of a 1 μm polyethylene terephthalate substrate.[46] In order to maintain flexibility and transparency, the electrode part is made of WO_3/Au/WO_3 (81% transparency) (Fig. 9c) for the detection of L-cysteine. In mechanical performance tests, it can be recovered after 100 deformations such as bending, folding and shrinking.

Fig. 9d shows another graphene aptamer nanobiosensor fabricated on a PET substrate.[139] Among them, polyethylenimide (PEI) is used for graphene surface antifouling, which can reach the LOD of hemoglobin (Hb) in human serum of 14.2 fM, and the sensor can also resist hundreds of cyclic stretching and bending strains.

Compared with photolithography, laser micromachining can quickly manufacture flexible electrodes and microstructure patterns. Furlan De Oliveira *et al.* produced an rGO liquid-gated transistor (LGT) using laser micromachining technology.[33] The sensing channels of rGO and an ion selective membrane (ISM) were functionalized (Fig. 9e) to obtain ion screening and fast response characteristics. It can operate at a low voltage (0.5 V) and has a linear response to K^+ and Na^+ in artificial sweat, and the detection concentration range is 10 μM–100 mM.

To enhance the functionality of the pressure sensor, Paul *et al.* affixed crumpled graphene onto a graphene–chitosan (GO–CS) substrate.[140] This sensor facilitates remote control of robot movement. When affixed to the temples of the face, it responds to facial muscle activity, generating a signal.

Moreover, the integration of sensors into wearable fabrics enables seamless real-time monitoring of human skin sweat for disease detection. Illustrated in Fig. 9f is a fabric composed of carbon nanotube/graphene (CNT/G) composite fibers.[48] This flexible fabric system is adaptable for wear on various body parts. Functionalizing the IL-6 aptamer within the fabric enables the detection of IL-6 in sweat.

Fig. 9g showcases a wearable contact lens designed for wireless communication and real-time detection of cortisol levels.[37] The sensor contains a graphene sensing channel, an NFC device, and a stretched antenna, which enables real-time host computer transmission of the detected concentration in tears. Notably, the contact lens boasts non-invasiveness, reliability, and good biocompatibility, validated through experiments conducted on living rabbits.

6. System-level integration of GFETs toward commercialization

Although some progress has been made with individual sensing systems, there is an eternal need to integrate more functional components into devices.[12,77,141,142] Commercial sensor systems usually require sensing units, communication, data processing, power supply and so on.[37,43] The miniaturization and integration of FET sensor systems can simplify the detection process and reduce weight and power consumption, while improving the detection stability and facilitating market applications.[41,143,144]

Fig. 10a shows the application of CRISPR technology to a GFET sensor and the anchoring of the Cas9 protein and graphene sensing channel to complete the modification.[78] In this work, rapid guidance of RNA–Cas9 complexes and detection of homozygous and heterozygous DNA samples were used to improve the efficiency of gene targeting in sickle cell patients.

Fig. 10b illustrates an integrated GFET sensor referred to as an EV chip.[141] The EV chip reader integrates multiplexer, microprocessor controller, potentiostat, and serial interface components. Through the modification of CD63 and CD151 probes, this EV chip enables the detection of plasma exosomes associated with age-related diseases, facilitating early diagnosis of conditions like Alzheimer's disease.

Kim *et al.* integrated an antibiotic-modified GFET and a microfluidic chip for clinical Gram-positive bacteria typing.[38] Notably, the portable sensor, depicted in Fig. 10c, incorporates a battery, communication module, microcontroller, and other components to achieve real-time transmission of detection signals. This setup achieves a LOD of 10 CFU mL^{-1} with minimized manual intervention.

During the COVID-19 pandemic, many researchers began to focus on creating miniaturized, integrated biosensors for biomarker diagnostics. Hao *et al.* employed Tween 80 for surface antifouling of GFET sensors to detect cytokines in biological fluids.[36] Illustrated in Fig. 10d is a biosensor device featuring an integrated OLED screen, wireless signal transmission, and a sensor signal acquisition module. This device is adept at detecting cytokines in patients and wirelessly transmitting the data to smartphones for early warning and reminders.

Fig. 10e shows a portable prototype device for SARS-CoV-2 detection,[39] which can detect and distinguish between COVID-19 negative and positive patients within 4 minutes. The portable prototype device integrates a controller, signal processing output module, rechargeable lithium battery and other components, which can be connected to smart phones or computers through USB, WiFi or Bluetooth.

Park *et al.* integrated RT-LAMP technology with crumpled graphene to develop a cgFET device for SARS-CoV-2 detection.[71] After isothermal amplification of the samples, cgFETs were employed for detection within a closed chamber, yielding results within 35 minutes. The platform (refer to Fig. 10f) demonstrates the capability to detect the virus within a concentration range of 10–10^4 copies per μL in virus transport medium.

Dai *et al.* integrated various antibodies on a GFET to capture the novel coronavirus with diverse configurations.[144] The results obtained from nasopharyngeal swabs showed approximately 100% consistency with the actual results, with a diagnostic time of less than 40 seconds in artificial saliva. The virus LOD can reach 3.5×10^{-11} μg mL^{-1}. Additionally, they developed a multi-antibody FET sensor packaged with a PCB substrate (depicted in Fig. 10g). This platform facilitates rapid, cost-effective, and high-precision antigen detection using either a single or a 10-in-1 mixed sample.

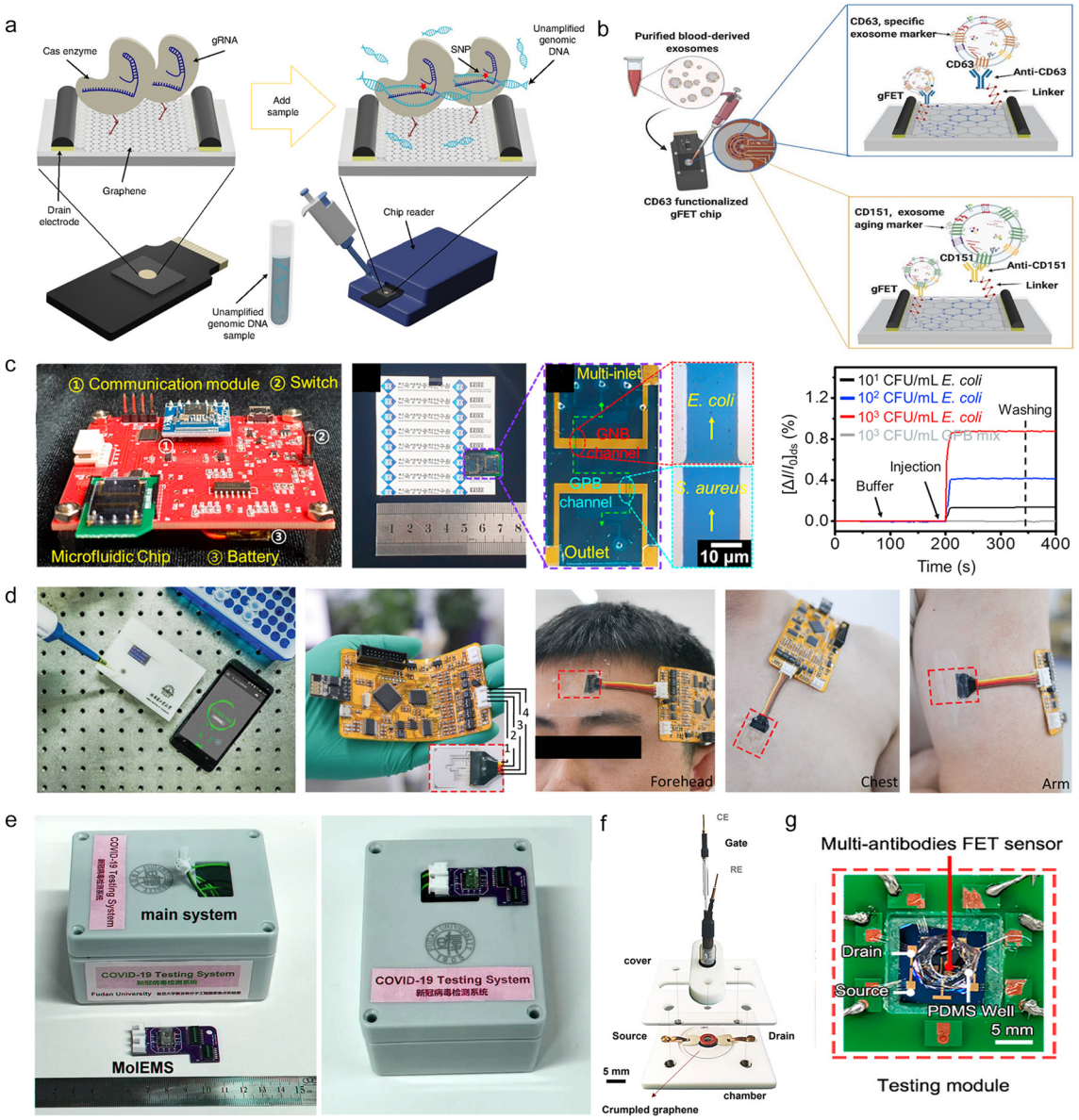

Fig. 10 System integration of GFETs toward commercialization. a) A Cas9-GFET that detects single-stranded DNA. Reproduced with permission.[78] Copyright 2021, *Nature Biomedical Engineering*. b) Schematic diagram of a microarray for the detection of plasma exosomes. Reproduced with permission.[141] Copyright 2021, *Advanced Biology*. c) Microfluidic chips for bacterial detection. Reproduced with permission.[38] Copyright 2020, *Biosensors and Bioelectronics*. d) A biosensing device for detection of cytokine. Reproduced with permission.[36] Copyright 2021 *Small*. e) Prototype of a COVID-19 virus detection system. The image shows the main system and the MolEMS g-FET testing module. Reproduced with permission.[39] Copyright 2022, *Nature Biomedical Engineering*. f) A microfluidic chamber using crumpled graphene as a sensing channel. Reproduced with permission.[71] Copyright 2021, *ACS Sensors*. g) Detection module of a multi-antibody FET sensor. Reproduced with permission.[144] Copyright 2021, *Journal of the American Chemical Society*.

Sections 4–6 summarize representative applications of GFET biosensors, including multiplex integrated arrays, flexible wearable applications, and system-level integrated devices. Table 2 presents a comparative analysis of the performance of the latest GFET biosensing applications, detailing aspects such as the selection of gate configuration strategies, anti-interference capabilities in the biosensing area, reproducibility across different batches of sensing devices, and the number of human subjects involved in proof-of-concept studies.

7. Challenges and future outlook

As an emerging sensing technology, GFET sensors have demonstrated exceptional capabilities in terms of biocompatibility, sensing performance, and potential system integration. For instance, traditional cytokine detection methods, such as ELISA[145,146] and immunofluorescence assays,[147–149] are commercially available and enable specific and sensitive detection. However, these commercial methods are often limited by labor-intensive, complex operations and

Table 2 Summary of sensing performance for GFET biosensing applications

Material	Target	LOD	Response time	Gate configurations	Robustness (interference target)	Reproducibility (device num.)	Human subjects	Year	Ref.
Graphene	Penicillin G	—	—	External Ag/AgCl gate	Urea	>35	—	19	44
Graphene	DNA	25 aM	40 min	Planar gate	SNP	>5	—	19	45
Graphene	SARS-CoV-2 antigen protein	1 fg mL^{-1}	—	External Ag/AgCl gate	MERS-CoV spike proteins	—	3	20	26
Graphene	Cortisol	10 pg ml^{-1}	—	External Ag/AgCl gate	Ascorbic acid, lactate, and urea	>10	1	20	37
Graphene	IFN-γ	476 fM	7 min	Planar gate	Insulin and IL-2	>3	2	21	36
Graphene	SARS-CoV-2 spike protein	0.173 copies per μL	20–72 s	Planar gate	—	5	38	21	144
Crumpled graphene	ssDNA	—	35 min	External Ag/AgCl gate	dsDNA	>3	20	21	71
Graphene	SARS-CoV-2 nucleic acid	0.02 copies per μL	0.1–4 min	Planar gate	Human cDNA and related coronavirus IVT RNA	15	87	22	39
Graphene	L-Cysteine	22 nM	—	Planar gate	D-Methionine, fmoc-L-tryptophan	>3	1	22	46
Graphene	Hemoglobin	14.2 fM	6–8 min	Planar gate	Lactate dehydrogenase, human creatine kinase MB	>3	—	22	139
Laser-engraved graphene	Leucine	—	7 min	Planar gate	Tryptophan, tyrosine, isoleucine and valine	12	26	22	124
rGO	K^+ and Na^+	—	5–15 s	Planar gate	Cl^-, NH_4^+	40	—	22	33
Graphene	HepG2 exosomes	242 particles per mL	9 min	External Ag/AgCl gate	—	3	14	23	47
Graphene	dsDNA	10 aM	30 min	External Ag/AgCl gate	SNP	48	—	23	49
Graphene	GPC-1 cancerous exosomes	—	45 min	Planar gate	Healthy exosomes	281	26	23	126
Carbon nanotube/graphene composite fibers	IL-6	280 fg mL^{-1}	3 min	Planar gate	BSA, HSA, DCD, IL-8	5	1	23	48

extended processing times. Additionally, label-free, highly sensitive, and specific detection techniques, including EIS[150,151] and differential pulse voltammetry (DPV),[152,153] have been widely employed in electrochemical biosensors. Despite these advancements, most detection techniques still require lengthy offline analysis and rely on complex instrumentation. Due to extensive research focused on wearable and portable integration, GFET biosensors are anticipated to form the foundation for future large-scale electronic applications sooner. In conclusion, we review and highlight the recent progress of GFET sensors and discuss how to improve the response of GFETs to detected substances through charge transfer or electrostatic induction, and on this basis, combined with a variety of gate configuration strategies, and achieve high sensitivity and high specificity marker detection on a single GFET device. In addition, multimodal detection of the same marker and cross-validation in multiplexing ensure the measurement reliability of GFETs, and the simultaneous detection of multiple markers also makes GFETs an important step in practical application. Wearable flexible GFET sensors are also often integrated with power supplies, communication modules, *etc.*, showing more conceptual application validation in neural interfaces, contact lenses, sewage treatment, *etc.* It is important to note that GFET biosensors are predominantly dependent on laboratory settings, with many applications remaining at the proof-of-concept stage. In this section, we enumerate several critical challenges and explore potential avenues for future research.

7.1 Standardization

In the realm of commercial medical diagnostics and health testing, both the exactitude and dependability of sensor detection results, alongside cost reduction, are paramount. Achieving these objectives necessitates standardized production and testing procedures. The problem faced by current mass production is how to obtain two-dimensional sensors with stable and consistent device performance. For large-scale production of GFET biosensors with consistent device quality, emphasis must be placed on the graphene growth process, including the use of CVD large-area growth technology and stringent control over manufacturing parameters to minimize

variations in channel materials. Additionally, securing high-density probe molecules on channel surfaces requires identifying an appropriate chemical coupling method to enhance sensor performance repeatability. Implementing surface antifouling strategies is crucial for maintaining sensor consistency. In the presence of complex fluids like saliva, blood, and urine, unspecific adsorption of contaminants at active sites diminishes GFET sensitivity. To address this issue, researchers have formulated various protocols, such as the use of bovine serum albumin (BSA),[39] PEI,[139] Tween 80,[138] and ethanolamine.[154] Moreover, the avoidance of toxic substances is essential for environmentally sustainable large-scale production. Standardization of sensor usage and result analysis procedures is also necessary to ensure accuracy and reproducibility of detection outcomes. Through the establishment of a comprehensive standardized process, GFET sensors can achieve device interchangeability and enhanced cost-effectiveness.

7.2 Artificial intelligence and regulation

Currently, the focus of GFET biosensors has gradually expanded from detecting single biomarkers to the simultaneous monitoring of multiple physiological parameters, which provides significantly richer data. To effectively analyze and process this vast amount of data, artificial intelligence (AI) and big data analytics have become increasingly integrated into the field.[3,121] For instance, multimodal data collected in real time from individuals consuming alcohol *via* electronic skin, when analyzed using machine learning algorithms, can accurately predict personalized behavioral responses.[155] With the global proliferation of smartphones, numerous smartphone applications have entered the biosensor field, and biosensing systems have progressively incorporated features such as data analysis, storage, and sharing. As GFET biosensors gather vast amounts of human physiological data, concerns over data usage and user privacy are becoming increasingly prominent. The disclosure of clinical data could subject patients to social challenges, such as unequal treatment from insurance companies. Therefore, regulators must establish clear guidelines on data privacy and security, standardize the processes for data usage and sharing, and enhance regulatory frameworks to facilitate the early widespread adoption of GFET biosensors.

7.3 Promotion of flexible wearable GFETs

Flexible GFET sensors are anticipated to be one of the most promising research directions in biosensing due to their remarkable elasticity, stretchability, portability, and close adherence to human skin. However, these flexible sensors currently face a significant challenge regarding long-term stability. Flexible sensing modules typically consist of multiple layers of flexible materials, each with differing fatigue resistance and elasticity. During actual use on the human body, these sensors inevitably experience mechanical stressors such as bending, stretching, and torsion, which can result in interface separation between materials, thereby significantly diminishing sensor performance and potentially causing damage. Additionally, over prolonged detection periods, environmental physical and chemical pressures, including temperature and humidity variations, can alter the material properties of the flexible sensor, affecting detection accuracy. To mitigate the issue of interface separation caused by disparate material properties, it is essential first to minimize the differences in mechanical properties between material layers by selecting materials with similar fatigue resistance and elasticity, thus facilitating sensor composite fabrication. Furthermore, developing adhesives with enhanced interfacial adhesion can enable effective structural interconnection of different materials, reducing the likelihood of interface separation and ensuring long-term comfort for the user. To address the issue of long-term sensor performance degradation, developing new materials that exhibit insensitivity to environmental pressures is a viable solution. Stability in flexible sensor systems can be progressively enhanced through the development and modification of emerging materials. Additionally, sensor modules can be encapsulated to minimize environmental noise and temporal drift. For instance, applying antifouling coatings, such as bovine serum albumin (BSA), effectively mitigates the non-specific adsorption of substances onto the sensor. Reasonable packaging is crucial to ensure the repeatability and reliability of flexible GFET biosensors.

In summary, GFET biosensors have significant prospects for personalized healthcare due to their ultra-high sensitivity, ease of integration, and high biocompatibility. Addressing key challenges such as standardized mass production, long-term stability, and responsible data utilization is essential to facilitate the commercialization process of GFET biosensors. In the foreseeable future, researchers will continue to advance GFET sensing systems with high reliability, biocompatibility, low power consumption, and cost-effectiveness, which are anticipated to be widely adopted across fields including wearable electronics, drug delivery, health monitoring, and healthcare.

Data availability

No primary research results, software or code have been included and no new data were generated or analysed as part of this review.

Conflicts of interest

There are no conflicts to declare.

Acknowledgements

This research was supported by the Natural Science Foundation of Heilongjiang Province (Grant No. YQ2022E23), the National Natural Science Foundation of China (Grant No.

51975145, 51975163, 52005137, and 52105571), the China Postdoctoral Science Foundation (Grant No. 2021TQ0087), and the Natural Science Foundation of Chongqing Municipality (Grant No. CSTB2023NSCQ-MSX0669).

References

1 N. N. Misra, Y. Dixit, A. Al-Mallahi, M. S. Bhullar, R. Upadhyay and A. Martynenko, IoT, Big Data, and Artificial Intelligence in Agriculture and Food Industry, *IEEE Internet Things J.*, 2022, **9**(9), 6305–6324.

2 A. G. Sreedevi, T. Nitya Harshitha, V. Sugumaran and P. Shankar, Application of cognitive computing in healthcare, cybersecurity, big data and IoT: A literature review, *Inf. Process. Manage.*, 2022, **59**(2), 102888.

3 X. Jin, C. Liu, T. Xu, L. Su and X. Zhang, Artificial intelligence biosensors: Challenges and prospects, *Biosens. Bioelectron.*, 2020, **165**, 112412.

4 C. Klumpp-Thomas, H. Kalish, M. Drew, S. Hunsberger, K. Snead, M. P. Fay, J. Mehalko, A. Shunmugavel, V. Wall, P. Frank, J. Denson, M. Hong, G. Gulten, S. Messing, J. Hicks, S. Michael, W. Gillette, M. D. Hall, M. J. Memoli, D. Esposito and K. Sadtler, Standardization of ELISA protocols for serosurveys of the SARS-CoV-2 pandemic using clinical and at-home blood sampling, *Nat. Commun.*, 2021, **12**(1), 113.

5 S. Platton, A. Bartlett, P. Maccallum, M. Makris, V. Mcdonald, D. Singh, M. Scully and S. Pavord, Evaluation of laboratory assays for anti-platelet factor 4 antibodies after ChAdOx1 nCOV-19 vaccination, *J. Thromb. Haemostasis*, 2021, **19**(8), 2007–2013.

6 M. Zhang, Y. Liu, D. Li, X. Cui, L. Wang, L. Li and K. Wang, Electrochemical Impedance Spectroscopy: A New Chapter in the Fast and Accurate Estimation of the State of Health for Lithium-Ion Batteries, *Energies*, 2023, **16**(4), 1599.

7 M. Gaberšček, Understanding Li-based battery materials via electrochemical impedance spectroscopy, *Nat. Commun.*, 2021, **12**(1), 6513.

8 Z. Huang, W. Wang, Y. Wang, H. Wang, Y. Pang, Q. Yuan, J. Tan and W. Tan, Electrochemical Detection of Viral Nucleic Acids by DNA Nanolock-Based Porous Electrode Device, *Anal. Chem.*, 2023, **95**(45), 16668–16676.

9 J. Plou, P. S. Valera, I. García, C. D. L. de Albuquerque, A. Carracedo and L. M. Liz-Marzán, Prospects of Surface-Enhanced Raman Spectroscopy for Biomarker Monitoring toward Precision Medicine, *ACS Photonics*, 2022, **9**(2), 333–350.

10 M. A. Tahir, N. E. Dina, H. Cheng, V. K. Valev and L. Zhang, Surface-enhanced Raman spectroscopy for bioanalysis and diagnosis, *Nanoscale*, 2021, **13**(27), 11593–11634.

11 Y. Song, L. Wang, T. Xu, G. Zhang and X. Zhang, Emerging open-channel droplet arrays for biosensing, *Natl. Sci. Rev.*, 2023, **10**(10), nwad106.

12 C. Dai, Y. Liu and D. Wei, Two-Dimensional Field-Effect Transistor Sensors: The Road toward Commercialization, *Chem. Rev.*, 2022, **122**(11), 10319–10392.

13 B. Wang, C. Zhao, Z. Wang, K. Yang, X. Cheng, W. Liu, W. Yu, S. Lin, Y. Zhao, K. M. Cheung, H. Lin, H. Hojaiji, P. S. Weiss, M. N. Stojanović, A. J. Tomiyama, A. M. Andrews and S. Emaminejad, Wearable aptamer-field-effect transistor sensing system for noninvasive cortisol monitoring, *Sci. Adv.*, 2022, **8**(1), eabk0967.

14 W. Shao, M. R. Shurin, S. E. Wheeler, X. He and A. Star, Rapid Detection of SARS-CoV-2 Antigens Using High-Purity Semiconducting Single-Walled Carbon Nanotube-Based Field-Effect Transistors, *ACS Appl. Mater. Interfaces*, 2021, **13**(8), 10321–10327.

15 P. Fathi-Hafshejani, N. Azam, L. Wang, M. A. Kuroda, M. C. Hamilton, S. Hasim and M. Mahjouri-Samani, Two-Dimensional-Material-Based Field-Effect Transistor Biosensor for Detecting COVID-19 Virus (SARS-CoV-2), *ACS Nano*, 2021, **15**(7), 11461–11469.

16 Y. Reddy, J. H. Shin, V. N. Palakollu, B. Sravani, C. H. Choi, K. Park, S. K. Kim, G. Madhavi, J. P. Park and N. P. Shetti, Strategies, advances, and challenges associated with the use of graphene-based nanocomposites for electrochemical biosensors, *Adv. Colloid Interface Sci.*, 2022, **304**, 102664.

17 S. Ullah, X. Yang, H. Q. Ta, M. Hasan, A. Bachmatiuk, K. Tokarska, B. Trzebicka, L. Fu and M. H. Rummeli, Graphene transfer methods: A review, *Nano Res.*, 2021, **14**(11), 3756–3772.

18 J. Bi, Z. Du, J. Sun, Y. Liu, K. Wang, H. Du, W. Ai and W. Huang, On the Road to the Frontiers of Lithium-Ion Batteries: A Review and Outlook of Graphene Anodes, *Adv. Mater.*, 2023, **35**(16), e2210734.

19 M. S. Ergoktas, G. Bakan, E. Kovalska, L. W. Le Fevre, R. P. Fields, P. Steiner, X. Yu, O. Salihoglu, S. Balci, V. I. Fal Ko, K. S. Novoselov, R. A. W. Dryfe and C. Kocabas, Multispectral graphene-based electro-optical surfaces with reversible tunability from visible to microwave wavelengths, *Nat. Photonics*, 2021, **15**(7), 493–498.

20 Y. Chen, J. Li, T. Li, L. Zhang and F. Meng, Recent advances in graphene-based films for electromagnetic interference shielding: Review and future prospects, *Carbon*, 2021, **180**, 163–184.

21 W. Fu, L. Feng, G. Panaitov, D. Kireev, D. Mayer, A. Offenhäusser and H. Krause, Biosensing near the neutrality point of graphene, *Sci. Adv.*, 2017, **3**(10), e1701247.

22 J. Li, M. Chen, A. Samad, H. Dong, A. Ray, J. Zhang, X. Jiang, U. Schwingenschlögl, J. Domke, C. Chen, Y. Han, T. Fritz, R. S. Ruoff, B. Tian and X. Zhang, Wafer-scale single-crystal monolayer graphene grown on sapphire substrate, *Nat. Mater.*, 2022, **21**(7), 740–747.

23 Y. Liu, X. Duan, H. J. Shin, S. Park, Y. Huang and X. Duan, Promises and prospects of two-dimensional transistors, *Nature*, 2021, **591**(7848), 43–53.

24 M. Wang, M. Huang, D. Luo, Y. Li, M. Choe, W. K. Seong, M. Kim, S. Jin, M. Wang, S. Chatterjee, Y. Kwon, Z. Lee and R. S. Ruoff, Single-crystal, large-area, fold-free monolayer graphene, *Nature*, 2021, **596**(7873), 519–524.

25 A. E. Islam, R. Martineau, C. M. Crasto, H. Kim, R. S. Rao, B. Maruyama, S. S. Kim and L. F. Drummy, Graphene-Based

Electrolyte-Gated Field-Effect Transistors for Potentiometrically Sensing Neuropeptide Y in Physiologically Relevant Environments, *ACS Appl. Nano Mater.*, 2020, **3**(6), 5088–5097.

26 G. Seo, G. Lee, M. J. Kim, S. Baek, M. Choi, K. B. Ku, C. Lee, S. Jun, D. Park, H. G. Kim, S. Kim, J. Lee, B. T. Kim, E. C. Park and S. I. Kim, Rapid Detection of COVID-19 Causative Virus (SARS-CoV-2) in Human Nasopharyngeal Swab Specimens Using Field-Effect Transistor-Based Biosensor, *ACS Nano*, 2020, **14**(4), 5135–5142.

27 J. Kim, J. Na, M. Joo and D. Suh, Low-Voltage-Operated Highly Sensitive Graphene Hall Elements by Ionic Gating, *ACS Appl. Mater. Interfaces*, 2019, **11**(4), 4226–4232.

28 N. C. S. Vieira, J. Borme, G. Machado, F. Cerqueira, P. P. Freitas, V. Zucolotto, N. M. R. Peres and P. Alpuim, Graphene field-effect transistor array with integrated electrolytic gates scaled to 200 mm, *J. Phys.: Condens. Matter*, 2016, **28**(8), 85302.

29 Z. Gao, H. Xia, J. Zauberman, M. Tomaiuolo, J. Ping, Q. Zhang, P. Ducos, H. Ye, S. Wang, X. Yang, F. Lubna, Z. Luo, L. Ren and A. T. C. Johnson, Detection of Sub-fM DNA with Target Recycling and Self-Assembly Amplification on Graphene Field-Effect Biosensors, *Nano Lett.*, 2018, **18**(6), 3509–3515.

30 F. Torricelli, D. Z. Adrahtas, Z. Bao, M. Berggren, F. Biscarini, A. Bonfiglio, C. A. Bortolotti, C. D. Frisbie, E. Macchia, G. G. Malliaras, I. Mcculloch, M. Moser, T. Nguyen, R. M. Owens, A. Salleo, A. Spanu and L. Torsi, Electrolyte-gated transistors for enhanced performance bioelectronics, *Nat. Rev. Methods Primers*, 2021, **1**(1), 66.

31 K. Tamersit, M. Kotti and M. Fakhfakh, A new pressure microsensor based on dual-gate graphene field-effect transistor with a vertically movable top-gate: Proposal, analysis, and optimization, *AEU-Int. J. Electron. Commun.*, 2020, **124**, 153346.

32 B. Hu, H. Sun, J. Tian, J. Mo, W. Xie, Q. M. Song, W. Zhang and H. Dong, Advances in flexible graphene field-effect transistors for biomolecule sensing, *Front. Bioeng. Biotechnol.*, 2023, **11**, 1218024.

33 R. Furlan De Oliveira, V. Montes García, P. A. Livio, M. B. González García, P. Fanjul Bolado, S. Casalini and P. Samorì, Selective Ion Sensing in Artificial Sweat Using Low-Cost Reduced Graphene Oxide Liquid-Gated Plastic Transistors, *Small*, 2022, **18**(27), 2201861.

34 J. Wang, L. Wang, G. Li, D. Yan, C. Liu, T. Xu and X. Zhang, Ultra-Small Wearable Flexible Biosensor for Continuous Sweat Analysis, *ACS Sens.*, 2022, **7**(10), 3102–3107.

35 H. Wang, Y. Wang, W. Wang, Y. Zhang, Q. Yuan and J. Tan, Materials-Functionalized Point-of-Care Testing Devices for Pathogen Detection, *Acc. Mater. Res.*, 2023, **4**(12), 1083–1094.

36 Z. Hao, Y. Luo, C. Huang, Z. Wang, G. Song, Y. Pan, X. Zhao and S. Liu, An Intelligent Graphene-Based Biosensing Device for Cytokine Storm Syndrome Biomarkers Detection in Human Biofluids, *Small*, 2021, **17**(29), 2101508.

37 M. Ku, J. Kim, J. Won, W. Kang, Y. Park, J. Park, J. Lee, J. Cheon, H. H. Lee and J. Park, Smart, soft contact lens for wireless immunosensing of cortisol, *Sci. Adv.*, 2020, **6**(28), eabb2891.

38 K. H. Kim, S. J. Park, C. S. Park, S. E. Seo, J. Lee, J. Kim, S. H. Lee, S. Lee, J. Kim, C. Ryu, D. Yong, H. Yoon, H. S. Song, S. H. Lee and O. S. Kwon, High-performance portable graphene field-effect transistor device for detecting Gram-positive and -negative bacteria, *Biosens. Bioelectron.*, 2020, **167**, 112514.

39 L. Wang, X. Wang, Y. Wu, M. Guo, C. Gu, C. Dai, D. Kong, Y. Wang, C. Zhang, D. Qu, C. Fan, Y. Xie, Z. Zhu, Y. Liu and D. Wei, Rapid and ultrasensitive electromechanical detection of ions, biomolecules and SARS-CoV-2 RNA in unamplified samples, *Nat. Biomed. Eng.*, 2022, **6**(3), 276–285.

40 C. Huang, W. Yang, H. Wang, S. Huang, S. Gao, D. Li, J. Liu, S. Hou, W. Feng, Z. Wang, F. Li, Z. Hao, X. Zhao, P. Hu and Y. Pan, Flexible/Regenerative Nanosensor with Automatic Sweat Collection for Cytokine Storm Biomarker Detection, *ACS Nano*, 2024, **18**(32), 21198–21210.

41 G. Ke, D. Su, Y. Li, Y. Zhao, H. Wang, W. Liu, M. Li, Z. Yang, F. Xiao, Y. Yuan, F. Huang, F. Mo, P. Wang and X. Guo, An accurate, high-speed, portable bifunctional electrical detector for COVID-19, *Sci. China Mater.*, 2021, **64**(3), 739–747.

42 Y. Luo, M. R. Abidian, J. H. Ahn, D. Akinwande, A. M. Andrews, M. Antonietti, Z. Bao, M. Berggren, C. A. Berkey, C. J. Bettinger, J. Chen, P. Chen, W. Cheng, X. Cheng, S. J. Choi, A. Chortos, C. Dagdeviren, R. H. Dauskardt, C. A. Di, M. D. Dickey, X. Duan, A. Facchetti, Z. Fan, Y. Fang, J. Feng, X. Feng, H. Gao, W. Gao, X. Gong, C. F. Guo, X. Guo, M. C. Hartel, Z. He, J. S. Ho, Y. Hu, Q. Huang, Y. Huang, F. Huo, M. M. Hussain, A. Javey, U. Jeong, C. Jiang, X. Jiang, J. Kang, D. Karnaushenko, A. Khademhosseini, D. H. Kim, I. D. Kim, D. Kireev, L. Kong, C. Lee, N. E. Lee, P. S. Lee, T. W. Lee, F. Li, J. Li, C. Liang, C. T. Lim, Y. Lin, D. J. Lipomi, J. Liu, K. Liu, N. Liu, R. Liu, Y. Liu, Y. Liu, Z. Liu, Z. Liu, X. J. Loh, N. Lu, Z. Lv, S. Magdassi, G. G. Malliaras, N. Matsuhisa, A. Nathan, S. Niu, J. Pan, C. Pang, Q. Pei, H. Peng, D. Qi, H. Ren, J. A. Rogers, A. Rowe, O. G. Schmidt, T. Sekitani, D. G. Seo, G. Shen, X. Sheng, Q. Shi, T. Someya, Y. Song, E. Stavrinidou, M. Su, X. Sun, K. Takei, X. M. Tao, B. Tee, A. V. Thean, T. Q. Trung, C. Wan, H. Wang, J. Wang, M. Wang, S. Wang, T. Wang, Z. L. Wang, P. S. Weiss, H. Wen, S. Xu, T. Xu, H. Yan, X. Yan, H. Yang, L. Yang, S. Yang, L. Yin, C. Yu, G. Yu, J. Yu, S. H. Yu, X. Yu, E. Zamburg, H. Zhang, X. Zhang, X. Zhang, X. Zhang, Y. Zhang, Y. Zhang, S. Zhao, X. Zhao, Y. Zheng, Y. Q. Zheng, Z. Zheng, T. Zhou, B. Zhu, M. Zhu, R. Zhu, Y. Zhu, Y. Zhu, G. Zou and X. Chen, Technology Roadmap for Flexible Sensors, *ACS Nano*, 2023, **17**(6), 5211–5295.

43 R. Garcia-Cortadella, G. Schwesig, C. Jeschke, X. Illa, A. L. Gray, S. Savage, E. Stamatidou, I. Schiessl, E. Masvidal-Codina, K. Kostarelos, A. Guimerà-Brunet, A. Sirota and J. A. Garrido, Graphene active sensor arrays for long-term

and wireless mapping of wide frequency band epicortical brain activity, *Nat. Commun.*, 2021, **12**(1), 211.

44 X. Dai, R. Vo, H. Hsu, P. Deng, Y. Zhang and X. Jiang, Modularized Field-Effect Transistor Biosensors, *Nano Lett.*, 2019, **19**(9), 6658–6664.

45 R. Campos, J. Borme, J. R. Guerreiro, Jr., G. Machado, M. F. Cerqueira, D. Y. Petrovykh and P. Alpuim, Attomolar Label-Free Detection of DNA Hybridization with Electrolyte-Gated Graphene Field-Effect Transistors, *ACS Sens.*, 2019, **4**(2), 286–293.

46 C. Huang, Z. Hao, Z. Wang, H. Wang, X. Zhao and Y. Pan, An Ultraflexible and Transparent Graphene-Based Wearable Sensor for Biofluid Biomarkers Detection, *Adv. Mater. Technol.*, 2022, **7**(6), 2101131.

47 Y. Chen, D. Kong, L. Qiu, Y. Wu, C. Dai, S. Luo, Z. Huang, Q. Lin, H. Chen, S. Xie, L. Geng, J. Zhao, W. Tan, Y. Liu and D. Wei, Artificial Nucleotide Aptamer-Based Field-Effect Transistor for Ultrasensitive Detection of Hepatoma Exosomes, *Anal. Chem.*, 2023, **95**(2), 1446–1453.

48 H. Chu, X. Hu, C. Lee, A. Zhang, Y. Ye, Y. Wang, Y. Chen, X. Yan, X. Wang, J. Wei, S. He and Y. Li, A wearable electrochemical fabric for cytokine monitoring, *Biosens. Bioelectron.*, 2023, **232**, 115301.

49 Z. Weng, Z. You, H. Li, G. Wu, Y. Song, H. Sun, A. Fradlin, C. Neal-Harris, M. Lin, X. Gao and Y. Zhang, CRISPR-Cas12a Biosensor Array for Ultrasensitive Detection of Unamplified DNA with Single-Nucleotide Polymorphic Discrimination, *ACS Sens.*, 2023, **8**(4), 1489–1499.

50 W. Fu, L. Jiang, E. P. van Geest, L. M. C. Lima and G. F. Schneider, Sensing at the Surface of Graphene Field-Effect Transistors, *Adv. Mater.*, 2017, **29**(6), 1603610.

51 J. Gao, C. Wang, C. Wang, Y. Chu, S. Wang, M. Y. Sun, H. Ji, Y. Gao, Y. Wang, Y. Han, F. Song, H. Liu, Y. Zhang and L. Han, Poly-l-Lysine-Modified Graphene Field-Effect Transistor Biosensors for Ultrasensitive Breast Cancer miRNAs and SARS-CoV-2 RNA Detection, *Anal. Chem.*, 2022, **94**(3), 1626–1636.

52 C. Ji, J. Wei, L. Zhang, X. Hou, J. Tan, Q. Yuan and W. Tan, Aptamer-Protein Interactions: From Regulation to Biomolecular Detection, *Chem. Rev.*, 2023, **123**(22), 12471–12506.

53 C. Dai, D. Kong, C. Chen, Y. Liu and D. Wei, Graphene Transistors for In Vitro Detection of Health Biomarkers, *Adv. Funct. Mater.*, 2023, **33**(31), 2301948.

54 Z. Hao, Z. Wang, Y. Li, Y. Zhu, X. Wang, C. G. De Moraes, Y. Pan, X. Zhao and Q. Lin, Measurement of cytokine biomarkers using an aptamer-based affinity graphene nanosensor on a flexible substrate toward wearable applications, *Nanoscale*, 2018, **10**(46), 21681–21688.

55 C. Wang, Y. Li, Y. Zhu, X. Zhou, Q. Lin and M. He, High-κ Solid-Gate Transistor Configured Graphene Biosensor with Fully Integrated Structure and Enhanced Sensitivity, *Adv. Funct. Mater.*, 2016, **26**(42), 7668–7678.

56 Y. Li, C. Wang, Y. Zhu, X. Zhou, Y. Xiang, M. He and S. Zeng, Fully integrated graphene electronic biosensor for label-free detection of lead (II) ion based on G-quadruplex structure-switching, *Biosens. Bioelectron.*, 2017, **89**, 758–763.

57 G. E. Fenoy, W. A. Marmisollé, O. Azzaroni and W. Knoll, Acetylcholine biosensor based on the electrochemical functionalization of graphene field-effect transistors, *Biosens. Bioelectron.*, 2020, **148**, 111796.

58 R. Wang, Y. Cao, H. Qu, Y. Wang and L. Zheng, Label-free detection of Cu(II) in fish using a graphene field-effect transistor gated by structure-switching aptamer probes, *Talanta*, 2022, **237**, 122965.

59 S. Farid, X. Meshik, M. Choi, S. Mukherjee, Y. Lan, D. Parikh, S. Poduri, U. Baterdene, C. Huang, Y. Y. Wang, P. Burke, M. Dutta and M. A. Stroscio, Detection of Interferon gamma using graphene and aptamer based FET-like electrochemical biosensor, *Biosens. Bioelectron.*, 2015, **71**, 294–299.

60 X. Wang, Z. Hao, T. R. Olsen, W. Zhang and Q. Lin, Measurements of aptamer–protein binding kinetics using graphene field-effect transistors, *Nanoscale*, 2019, **11**(26), 12573–12581.

61 Z. Hao, Y. Zhu, X. Wang, P. G. Rotti, C. Dimarco, S. R. Tyler, X. Zhao, J. F. Engelhardt, J. Hone and Q. Lin, Real-Time Monitoring of Insulin Using a Graphene Field-Effect Transistor Aptameric Nanosensor, *ACS Appl. Mater. Interfaces*, 2017, **9**(33), 27504–27511.

62 Y. Zhu, C. Wang, N. Petrone, J. Yu, C. Nuckolls, J. Hone and Q. Lin, A solid dielectric gated graphene nanosensor in electrolyte solutions, *Appl. Phys. Lett.*, 2015, **106**(12), 123503.

63 X. Chen, Y. Liu, X. Fang, Z. Li, H. Pu, J. Chang, J. Chen and S. Mao, Ultratrace antibiotic sensing using aptamer/graphene-based field-effect transistors, *Biosens. Bioelectron.*, 2019, **126**, 664–671.

64 Z. Hao, Y. Pan, C. Huang, Z. Wang and X. Zhao, Sensitive detection of lung cancer biomarkers using an aptameric graphene-based nanosensor with enhanced stability, *Biomed. Microdevices*, 2019, **21**(3), 65.

65 Y. Zhang, D. Chen, W. He, N. Chen, L. Zhou, L. Yu, Y. Yang and Q. Yuan, Interface-Engineered Field-Effect Transistor Electronic Devices for Biosensing, *Adv. Mater.*, 2023, e2306252.

66 Y. Yang, J. Wang, W. Huang, G. Wan, M. Xia, D. Chen, Y. Zhang, Y. Wang, F. Guo, J. Tan, H. Liang, B. Du, L. Yu, W. Tan, X. Duan and Q. Yuan, Integrated Urinalysis Devices Based on Interface-Engineered Field-Effect Transistor Biosensors Incorporated With Electronic Circuits, *Adv. Mater.*, 2022, **34**(36), 2203224.

67 M. Deng, J. Li, B. Xiao, Z. Ren, Z. Li, H. Yu, J. Li, J. Wang, Z. Chen and X. Wang, Ultrasensitive Label-Free DNA Detection Based on Solution-Gated Graphene Transistors Functionalized with Carbon Quantum Dots, *Anal. Chem.*, 2022, **94**(7), 3320–3327.

68 S. Wang, M. Sun, Y. Zhang, H. Ji, J. Gao, S. Song, J. Sun, H. Liu, Y. Zhang and L. Han, Ultrasensitive Antibiotic Perceiving Based on Aptamer-Functionalized Ultraclean Graphene Field-Effect Transistor Biosensor, *Anal. Chem.*, 2022, **94**(42), 14785–14793.

69 Y. Wei, S. Long, M. Zhao, J. Zhao, Y. Zhang, W. He, L. Xiang, J. Tan, M. Ye, W. Tan, Y. Yang and Q. Yuan, Regulation of Cellular Signaling with an Aptamer Inhibitor to Impede Cancer Metastasis, *J. Am. Chem. Soc.*, 2024, **146**(1), 319–329.
70 D. Kong, X. Wang, C. Gu, M. Guo, Y. Wang, Z. Ai, S. Zhang, Y. Chen, W. Liu, Y. Wu, C. Dai, Q. Guo, D. Qu, Z. Zhu, Y. Xie, Y. Liu and D. Wei, Direct SARS-CoV-2 Nucleic Acid Detection by Y-Shaped DNA Dual-Probe Transistor Assay, *J. Am. Chem. Soc.*, 2021, **143**(41), 17004–17014.
71 I. Park, J. Lim, S. You, M. T. Hwang, J. Kwon, K. Koprowski, S. Kim, J. Heredia, S. A. Stewart De Ramirez, E. Valera and R. Bashir, Detection of SARS-CoV-2 Virus Amplification Using a Crumpled Graphene Field-Effect Transistor Biosensor, *ACS Sens.*, 2021, **6**(12), 4461–4470.
72 M. T. Hwang, M. Heiranian, Y. Kim, S. You, J. Leem, A. Taqieddin, V. Faramarzi, Y. Jing, I. Park, A. M. van der Zande, S. Nam, N. R. Aluru and R. Bashir, Ultrasensitive detection of nucleic acids using deformed graphene channel field effect biosensors, *Nat. Commun.*, 2020, **11**(1), 1543.
73 S. Ramadan, R. Lobo, Y. Zhang, L. Xu, O. Shaforost, D. Kwong Hong Tsang, J. Feng, T. Yin, M. Qiao, A. Rajeshirke, L. R. Jiao, P. K. Petrov, I. E. Dunlop, M. Titirici and N. Klein, Carbon-Dot-Enhanced Graphene Field-Effect Transistors for Ultrasensitive Detection of Exosomes, *ACS Appl. Mater. Interfaces*, 2021, **13**(7), 7854–7864.
74 Y. Li, Z. Peng, N. J. Holl, M. R. Hassan, J. M. Pappas, C. Wei, O. H. Izadi, Y. Wang, X. Dong, C. Wang, Y. Huang, D. Kim and C. Wu, MXene–Graphene Field-Effect Transistor Sensing of Influenza Virus and SARS-CoV-2, *ACS Omega*, 2021, **6**(10), 6643–6653.
75 H. Kang, X. Wang, M. Guo, C. Dai, R. Chen, L. Yang, Y. Wu, T. Ying, Z. Zhu, D. Wei, Y. Liu and D. Wei, Ultrasensitive Detection of SARS-CoV-2 Antibody by Graphene Field-Effect Transistors, *Nano Lett.*, 2021, **21**(19), 7897–7904.
76 T. Rodrigues, F. Curti, Y. R. Leroux, A. Barras, Q. Pagneux, H. Happy, C. Kleber, R. Boukherroub, R. Hasler, S. Volpi, M. Careri, R. Corradini, S. Szunerits and W. Knoll, Discovery of a Peptide Nucleic Acid (PNA) aptamer for cardiac troponin I: Substituting DNA with neutral PNA maintains picomolar affinity and improves performances for electronic sensing with graphene field-effect transistors (gFET), *Nano Today*, 2023, **50**, 101840.
77 R. Hajian, S. Balderston, T. Tran, T. Deboer, J. Etienne, M. Sandhu, N. A. Wauford, J. Chung, J. Nokes, M. Athaiya, J. Paredes, R. Peytavi, B. Goldsmith, N. Murthy, I. M. Conboy and K. Aran, Detection of unamplified target genes via CRISPR–Cas9 immobilized on a graphene field-effect transistor, *Nat. Biomed. Eng.*, 2019, **3**(6), 427–437.
78 S. Balderston, J. J. Taulbee, E. Celaya, K. Fung, A. Jiao, K. Smith, R. Hajian, G. Gasiunas, S. Kutanovas, D. Kim, J. Parkinson, K. Dickerson, J. Ripoll, R. Peytavi, H. Lu, F. Barron, B. R. Goldsmith, P. G. Collins, I. M. Conboy, V. Siksnys and K. Aran, Discrimination of single-point mutations in unamplified genomic DNA via Cas9 immobilized on a graphene field-effect transistor, *Nat. Biomed. Eng.*, 2021, **5**(7), 713–725.
79 C. Wang, Y. Li, Y. Zhu, X. Zhou, Q. Lin and M. He, High-κ Solid-Gate Transistor Configured Graphene Biosensor with Fully Integrated Structure and Enhanced Sensitivity, *Adv. Funct. Mater.*, 2016, **26**(47), 8575.
80 J. Xiao, C. Fan, T. Xu, L. Su and X. Zhang, An electrochemical wearable sensor for levodopa quantification in sweat based on a metal–Organic framework/graphene oxide composite with integrated enzymes, *Sens. Actuators, B*, 2022, **359**, 131586.
81 N. Yogeswaran, E. S. Hosseini and R. Dahiya, Graphene Based Low Voltage Field Effect Transistor Coupled with Biodegradable Piezoelectric Material Based Dynamic Pressure Sensor, *ACS Appl. Mater. Interfaces*, 2020, **12**(48), 54035–54040.
82 N. I. Khan, M. Mousazadehkasin, S. Ghosh, J. G. Tsavalas and E. Song, An integrated microfluidic platform for selective and real-time detection of thrombin biomarkers using a graphene FET, *Analyst*, 2020, **145**(13), 4494–4503.
83 N. Kumar, M. Rana, M. Geiwitz, N. I. Khan, M. Catalano, J. C. Ortiz-Marquez, H. Kitadai, A. Weber, B. Dweik, X. Ling, T. van Opijnen, A. A. Argun and K. S. Burch, Rapid, Multianalyte Detection of Opioid Metabolites in Wastewater, *ACS Nano*, 2022, **16**(3), 3704–3714.
84 L. Xu, S. Ramadan, O. E. Akingbade, Y. Zhang, S. Alodan, N. Graham, K. A. Zimmerman, E. Torres, A. Heslegrave, P. K. Petrov, H. Zetterberg, D. J. Sharp, N. Klein and B. Li, Detection of Glial Fibrillary Acidic Protein in Patient Plasma Using On-Chip Graphene Field-Effect Biosensors, in Comparison with ELISA and Single-Molecule Array, *ACS Sens.*, 2022, **7**(1), 253–262.
85 M. Deng, Z. Ren, H. Zhang, Z. Li, C. Xue, J. Wang, D. Zhang, H. Yang, X. Wang and J. Li, Unamplified and Real-Time Label-Free miRNA-21 Detection Using Solution-Gated Graphene Transistors in Prostate Cancer Diagnosis, *Adv. Sci.*, 2023, **10**(4), 2205886.
86 H. Zhang, H. Yu, M. Deng, Z. Ren, Z. Li, L. Zhang, J. Li, E. Wang, X. Wang and J. Li, Highly sensitive and real-time detection of sialic acid using a solution-gated graphene transistor functionalized with carbon quantum dots, *Microchem. J.*, 2023, **190**, 108676.
87 Z. Gao, H. Kang, C. H. Naylor, F. Streller, P. Ducos, M. D. Serrano, J. Ping, J. Zauberman, Rajesh, R. W. Carpick, Y. Wang, Y. W. Park, Z. Luo, L. Ren and A. T. C. Johnson, Scalable Production of Sensor Arrays Based on High-Mobility Hybrid Graphene Field Effect Transistors, *ACS Appl. Mater. Interfaces*, 2016, **8**(41), 27546–27552.
88 S. Ma, X. Li, Y. Lee and A. Zhang, Direct label-free protein detection in high ionic strength solution and human plasma using dual-gate nanoribbon-based ion-sensitive field-effect transistor biosensor, *Biosens. Bioelectron.*, 2018, **117**, 276–282.
89 Z. Hao, Y. Pan, W. Shao, Q. Lin and X. Zhao, Graphene-based fully integrated portable nanosensing system for on-line detection of cytokine biomarkers in saliva, *Biosens. Bioelectron.*, 2019, **134**, 16–23.

90 C. Huang, W. Huang, T. Huang, S. Ciou, C. Kuo, A. Hsieh, Y. Hsiao and Y. Lee, Dual-Gate Enhancement of the Sensitivity of miRNA Detection of a Solution-Gated Field-Effect Transistor Featuring a Graphene Oxide/Graphene Layered Structure, *ACS Appl. Electron. Mater.*, 2021, **3**(10), 4300–4307.

91 J. Li, A. Tyagi, T. Huang, H. Liu, H. Sun, J. You, M. M. Alam, X. Li and Z. Gao, Aptasensors Based on Graphene Field-Effect Transistors for Arsenite Detection, *ACS Appl. Nano Mater.*, 2022, **5**(9), 12848–12854.

92 M. Farahmandpour, H. Haghshenas and Z. Kordrostami, Blood glucose sensing by back gated transistor strips sensitized by CuO hollow spheres and rGO, *Sci. Rep.*, 2022, **12**(1), 21872.

93 D. Kwong Hong Tsang, T. J. Lieberthal, C. Watts, I. E. Dunlop, S. Ramadan, A. E. Del Rio Hernandez and N. Klein, Chemically Functionalised Graphene FET Biosensor for the Label-free Sensing of Exosomes, *Sci. Rep.*, 2019, **9**(1), 13946.

94 Z. Wang, Z. Zhang, H. Xu, L. Ding, S. Wang and L. Peng, A high-performance top-gate graphene field-effect transistor based frequency doubler, *Appl. Phys. Lett.*, 2010, **96**(17), 173104.

95 J. Gun Oh, S. Ki Hong, C. Kim, J. Hoon Bong, J. Shin, S. Choi and B. Jin Cho, High performance graphene field effect transistors on an aluminum nitride substrate with high surface phonon energy, *Appl. Phys. Lett.*, 2014, **104**(19), 193112.

96 Y. Sabir and S. M. Chaudhry, Modeling and Characterization of a Top Gated Graphene FET for RF Applications, *Proc. Natl. Acad. Sci., India, Sect. A*, 2018, **88**(2), 317–323.

97 M. K. Anvarifard, Z. Ramezani and I. S. Amiri, Label-free detection of DNA by a dielectric modulated armchair-graphene nanoribbon FET based biosensor in a dual-nanogap setup, *Mater. Sci. Eng., C*, 2020, **117**, 111293.

98 M. K. Anvarifard, Z. Ramezani and I. S. Amiri, Proposal of an Embedded Nanogap Biosensor by a Graphene Nanoribbon Field-Effect Transistor for Biological Samples Detection, *Phys. Status Solidi A*, 2020, **217**(2), 1900879.

99 E. H. Kim, D. H. Lee, T. J. Gu, H. Yoo, Y. Jang, J. Jeong, H. Kim, S. Kang, H. Kim, H. Lee, K. Jo, B. J. Kim, J. W. Kim, S. H. Im, C. S. Oh, C. Lee, K. K. Kim, C. Yang, H. Kim, Y. Kim, P. Kim, D. Whang and J. R. Ahn, Wafer-Scale Epitaxial Growth of an Atomically Thin Single-Crystal Insulator as a Substrate of Two-Dimensional Material Field-Effect Transistors, *Nano Lett.*, 2023, **23**(7), 3054–3061.

100 K. Yoshioka, T. Wakamura, M. Hashisaka, K. Watanabe, T. Taniguchi and N. Kumada, Ultrafast intrinsic optical-to-electrical conversion dynamics in a graphene photodetector, *Nat. Photonics*, 2022, **16**(10), 718–723.

101 M. W. Jung, W. Song, W. J. Choi, D. S. Jung, Y. J. Chung, S. Myung, S. S. Lee, J. Lim, C. Park, J. Lee and K. An, Fabrication of free-standing Al2O3 nanosheets for high mobility flexible graphene field effect transistors, *J. Mater. Chem. C*, 2014, **2**(24), 4759.

102 B. Hwang, H. Yeom, D. Kim, C. Kim, D. Lee and Y. Choi, Enhanced transconductance in a double-gate graphene field-effect transistor, *Solid-State Electron.*, 2018, **141**, 65–68.

103 H. Wu, Y. Cui, J. Xu, Z. Yan, Z. Xie, Y. Hu and S. Zhu, Multifunctional Half-Floating-Gate Field-Effect Transistor Based on MoS2–BN–Graphene van der Waals Heterostructures, *Nano Lett.*, 2022, **22**(6), 2328–2333.

104 X. Gao, X. She, C. Liu, Q. Sun, J. Liu and S. Wang, Organic field-effect transistor nonvolatile memories based on hybrid nano-floating-gate, *Appl. Phys. Lett.*, 2013, **102**(2), 023303.

105 M. Sup Choi, G. Lee, Y. Yu, D. Lee, S. Hwan Lee, P. Kim, J. Hone and W. Jong Yoo, Controlled charge trapping by molybdenum disulphide and graphene in ultrathin heterostructured memory devices, *Nat. Commun.*, 2013, **4**(1), 1624.

106 B. Hafsi, A. Boubaker, D. Guerin, S. Lenfant, A. Kalboussi and K. Lmimouni, N-type polymeric organic flash memory device: Effect of reduced graphene oxide floating gate, *Org. Electron.*, 2017, **45**, 81–88.

107 D. Svintsov, V. G. Leiman, V. Ryzhii, T. Otsuji and M. S. Shur, Graphene nanoelectromechanical resonators for the detection of modulated terahertz radiation, *J. Phys. D: Appl. Phys.*, 2014, **47**(50), 505101–505105.

108 Z. Sheng, J. Dong, W. Hu, Y. Wang, H. Sun, D. W. Zhang, P. Zhou and Z. Zhang, Reconfigurable Logic-in-Memory Computing Based on a Polarity-Controllable Two-Dimensional Transistor, *Nano Lett.*, 2023, **23**(11), 5242–5249.

109 S. Sheibani, L. Capua, S. Kamaei, S. S. A. Akbari, J. Zhang, H. Guerin and A. M. Ionescu, Extended gate field-effect-transistor for sensing cortisol stress hormone, *Commun. Mater.*, 2021, **2**(1), 10.

110 H. Jang, X. Sui, W. Zhuang, X. Huang, M. Chen, X. Cai, Y. Wang, B. Ryu, H. Pu, N. Ankenbruck, K. Beavis, J. Huang and J. Chen, Remote Floating-Gate Field-Effect Transistor with 2-Dimensional Reduced Graphene Oxide Sensing Layer for Reliable Detection of SARS-CoV-2 Spike Proteins, *ACS Appl. Mater. Interfaces*, 2022, **14**(21), 24187–24196.

111 H. Jang, W. Zhuang, X. Sui, B. Ryu, X. Huang, M. Chen, X. Cai, H. Pu, K. Beavis, J. Huang and J. Chen, Rapid, Sensitive, Label-Free Electrical Detection of SARS-CoV-2 in Nasal Swab Samples, *ACS Appl. Mater. Interfaces*, 2023, **15**(12), 15195–15202.

112 C. Wang, J. Wu, Y. He, Z. Song, S. Shi, Y. Zhu, Y. Jia and W. Ye, Fully Solid-State Graphene Transistors with Striking Homogeneity and Sensitivity for the Practicalization of Single-Device Electronic Bioassays, *Nano Lett.*, 2020, **20**(1), 166–175.

113 C. Mackin and T. Palacios, Large-scale sensor systems based on graphene electrolyte-gated field-effect transistors, *Analyst*, 2016, **141**(9), 2704–2711.

114 G. Zhong, Q. Liu, Q. Wang, H. Qiu, H. Li and T. Xu, Fully integrated microneedle biosensor array for wearable multiplexed fitness biomarkers monitoring, *Biosens. Bioelectron.*, 2024, **265**, 116697.

115 W. Gao, S. Emaminejad, H. Y. Y. Nyein, S. Challa, K. Chen, A. Peck, H. M. Fahad, H. Ota, H. Shiraki, D. Kiriya, D. Lien, G. A. Brooks, R. W. Davis and A. Javey, Fully integrated wearable sensor arrays for multiplexed in situ perspiration analysis, *Nature*, 2016, **529**(7587), 509–514.

116 H. E. Kim, A. Schuck, J. H. Lee and Y. Kim, Solution-gated graphene field effect transistor for TP53 DNA sensor with coplanar electrode array, *Sens. Actuators, B*, 2019, **291**, 96–101.

117 K. Mensah, I. Cissé, A. Pierret, M. Rosticher, J. Palomo, P. Morfin, B. Plaçais and U. Bockelmann, DNA Hybridization Measured with Graphene Transistor Arrays, *Adv. Healthcare Mater.*, 2020, **9**(16), 2000260.

118 G. Xu, J. Abbott, L. Qin, K. Y. M. Yeung, Y. Song, H. Yoon, J. Kong and D. Ham, Electrophoretic and field-effect graphene for all-electrical DNA array technology, *Nat. Commun.*, 2014, **5**(1), 4866.

119 S. Xu, J. Zhan, B. Man, S. Jiang, W. Yue, S. Gao, C. Guo, H. Liu, Z. Li, J. Wang and Y. Zhou, Real-time reliable determination of binding kinetics of DNA hybridization using a multi-channel graphene biosensor, *Nat. Commun.*, 2017, **8**(1), 14902.

120 F. Zou, Y. Luo, W. Zhuang and T. Xu, A Fully Integrated Conformal Wearable Ultrasound Patch for Continuous Sonodynamic Therapy, *Adv. Mater.*, 2024, e2409528.

121 Z. Zhou, X. He, J. Xiao, J. Pan, M. Li, T. Xu and X. Zhang, Machine learning-powered wearable interface for distinguishable and predictable sweat sensing, *Biosens. Bioelectron.*, 2024, **265**, 116712.

122 I. Fakih, O. Durnan, F. Mahvash, I. Napal, A. Centeno, A. Zurutuza, V. Yargeau and T. Szkopek, Selective ion sensing with high resolution large area graphene field effect transistor arrays, *Nat. Commun.*, 2020, **11**(1), 3226.

123 D. Park, J. H. Kim, H. J. Kim, D. Lee, D. S. Lee, D. S. Yoon and K. S. Hwang, Multiplexed femtomolar detection of Alzheimer's disease biomarkers in biofluids using a reduced graphene oxide field-effect transistor, *Biosens. Bioelectron.*, 2020, **167**, 112505.

124 M. Wang, Y. Yang, J. Min, Y. Song, J. Tu, D. Mukasa, C. Ye, C. Xu, N. Heflin, J. S. Mccune, T. K. Hsiai, Z. Li and W. Gao, A wearable electrochemical biosensor for the monitoring of metabolites and nutrients, *Nat. Biomed. Eng.*, 2022, **6**(11), 1225–1235.

125 V. Dupuit, O. Terral, G. Bres, A. Claudel, B. Fernandez, A. Briançon-Marjollet and C. Delacour, A Multifunctional Hybrid Graphene and Microfluidic Platform to Interface Topological Neuron Networks, *Adv. Funct. Mater.*, 2022, **32**(49), 2207001.

126 T. Yin, L. Xu, B. Gil, N. Merali, M. S. Sokolikova, D. C. A. Gaboriau, D. S. K. Liu, A. N. Muhammad Mustafa, S. Alodan, M. Chen, O. Txoperena, M. Arrastua, J. M. Gomez, N. Ontoso, M. Elicegui, E. Torres, D. Li, C. Mattevi, A. E. Frampton, L. R. Jiao, S. Ramadan and N. Klein, Graphene Sensor Arrays for Rapid and Accurate Detection of Pancreatic Cancer Exosomes in Patients' Blood Plasma Samples, *ACS Nano*, 2023, **17**(15), 14619–14631.

127 Z. Gao, P. Ducos, H. Ye, J. Zauberman, A. Sriram, X. Yang, Z. Wang, M. W. Mitchell, D. Lekkas, D. Brisson and A. T. C. Johnson, Graphene transistor arrays functionalized with genetically engineered antibody fragments for Lyme disease diagnosis, *2D Mater.*, 2020, **7**(2), 24001.

128 N. Gao, R. Zhou, B. Tu, T. Tao, Y. Song, Z. Cai, H. He, G. Chang, Y. Wu and Y. He, Graphene electrochemical transistor incorporated with gel electrolyte for wearable and non-invasive glucose monitoring, *Anal. Chim. Acta*, 2023, **1239**, 340719.

129 J. Xiao, Z. Zhou, G. Zhong, T. Xu and X. Zhang, Self-Sterilizing Microneedle Sensing Patches for Machine Learning-Enabled Wound pH Visual Monitoring, *Adv. Funct. Mater.*, 2024, **34**(22), 2315067.

130 H. C. Ates, P. Q. Nguyen, L. Gonzalez-Macia, E. Morales-Narváez, F. Güder, J. J. Collins and C. Dincer, End-to-end design of wearable sensors, *Nat. Rev. Mater.*, 2022, **7**(11), 887–907.

131 Z. Hao, Z. Wang, Y. Li, Y. Zhu, X. Wang, C. G. De Moraes, Y. Pan, X. Zhao and Q. Lin, Measurement of cytokine biomarkers using an aptamer-based affinity graphene nanosensor on a flexible substrate toward wearable applications, *Nanoscale*, 2018, **10**(46), 21681–21688.

132 Z. Wang, Z. Hao, S. Yu, C. G. De Moraes, L. H. Suh, X. Zhao and Q. Lin, An Ultraflexible and Stretchable Aptameric Graphene Nanosensor for Biomarker Detection and Monitoring, *Adv. Funct. Mater.*, 2019, **29**(44), 1905202.

133 C. Huang, Z. Hao, T. Qi, Y. Pan and X. Zhao, An integrated flexible and reusable graphene field effect transistor nanosensor for monitoring glucose, *J. Materiomics*, 2020, **6**(2), 308–314.

134 R. Furlan De Oliveira, P. A. Livio, V. Montes García, S. Ippolito, M. Eredia, P. Fanjul Bolado, M. B. González García, S. Casalini and P. Samorì, Liquid-Gated Transistors Based on Reduced Graphene Oxide for Flexible and Wearable Electronics, *Adv. Funct. Mater.*, 2019, **29**(46), 1905375.

135 J. W. Kim, S. Kim, Y. Jang, K. Lim and W. H. Lee, Attomolar detection of virus by liquid coplanar-gate graphene transistor on plastic, *Nanotechnology*, 2019, **30**(34), 345502.

136 C. Huang, D. Li, J. Liu, S. Hou, W. Yang, H. Wang, J. Wang, Z. Wang, F. Li, Z. Hao, S. Huang, X. Zhao, P. Hu and Y. Pan, A Flexible Aptameric Graphene Field-Effect Nanosensor Capable of Automatic Liquid Collection/Filtering for Cytokine Storm Biomarker Monitoring in Undiluted Sweat, *Adv. Funct. Mater.*, 2024, **34**(9), 2309447.

137 Q. Wang, Q. Liu, G. Zhong, T. Xu and X. Zhang, Wearable Vertical Graphene-Based Microneedle Biosensor for Real-Time Ketogenic Diet Management, *Anal. Chem.*, 2024, **96**(21), 8713–8720.

138 Z. Wang, Z. Hao, S. Yu, C. Huang, Y. Pan and X. Zhao, A Wearable and Deformable Graphene-Based Affinity Nanosensor for Monitoring of Cytokines in Biofluids, *Nanomaterials*, 2020, **10**(8), 1503.

139 Z. Hao, C. Huang, C. Zhao, A. Kospan, Z. Wang, F. Li, H. Wang, X. Zhao, Y. Pan and S. Liu, Ultrasensitive Graphene-

Based Nanobiosensor for Rapid Detection of Hemoglobin in Undiluted Biofluids, *ACS Appl. Bio Mater.*, 2022, **5**(4), 1624–1632.

140 A. Paul, N. Yogeswaran and R. Dahiya, Ultra-Flexible Biodegradable Pressure Sensitive Field Effect Transistors for Hands-Free Control of Robot Movements, *Adv. Intell. Syst.*, 2022, **4**(11), 2200183.

141 R. Hajian, J. Decastro, J. Parkinson, A. Kane, A. F. R. Camelo, P. P. Chou, J. Yang, N. Wong, E. D. O. Hernandez, B. Goldsmith, I. Conboy and K. Aran, Rapid and Electronic Identification and Quantification of Age-Specific Circulating Exosomes via Biologically Activated Graphene Transistors, *Adv. Biol.*, 2021, **5**(7), 2000594.

142 L. Wang, Y. Luo, Y. Song, X. He, T. Xu and X. Zhang, Hydrogel-Functionalized Bandages with Janus Wettability for Efficient Unidirectional Drug Delivery and Wound Care, *ACS Nano*, 2024, **18**(4), 3468–3479.

143 N. Mandal, V. Pakira, N. Samanta, N. Das, S. Chakraborty, B. Pramanick and C. Roychaudhuri, PSA detection using label free graphene FET with coplanar electrodes based microfluidic point of care diagnostic device, *Talanta*, 2021, **222**, 121581.

144 C. Dai, M. Guo, Y. Wu, B. Cao, X. Wang, Y. Wu, H. Kang, D. Kong, Z. Zhu, T. Ying, Y. Liu and D. Wei, Ultraprecise Antigen 10-in-1 Pool Testing by Multiantibodies Transistor Assay, *J. Am. Chem. Soc.*, 2021, **143**(47), 19794–19801.

145 P. M. Ridker, J. G. Macfadyen, T. Thuren and P. Libby, Residual inflammatory risk associated with interleukin-18 and interleukin-6 after successful interleukin-1β inhibition with canakinumab: further rationale for the development of targeted anti-cytokine therapies for the treatment of atherothrombosis, *Eur. Heart J.*, 2020, **41**(23), 2153–2163.

146 N. D'Onofrio, F. Prattichizzo, R. Marfella, C. Sardu, E. Martino, L. Scisciola, L. Marfella, R. L. Grotta, C. Frigé, G. Paolisso, A. Ceriello and M. L. Balestrieri, SIRT3 mediates the effects of PCSK9 inhibitors on inflammation, autophagy, and oxidative stress in endothelial cells, *Theranostics*, 2023, **13**(2), 531–542.

147 H. Zhu, Z. Jian, Y. Zhong, Y. Ye, Y. Zhang, X. Hu, B. Pu, L. Gu and X. Xiong, Janus Kinase Inhibition Ameliorates Ischemic Stroke Injury and Neuroinflammation Through Reducing NLRP3 Inflammasome Activation via JAK2/STAT3 Pathway Inhibition, *Front. Immunol.*, 2021, **12**, 714943.

148 M. Zhang, H. Yang, L. Wan, Z. Wang, H. Wang, C. Ge, Y. Liu, Y. Hao, D. Zhang, G. Shi, Y. Gong, Y. Ni, C. Wang, Y. Zhang, J. Xi, S. Wang, L. Shi, L. Zhang, W. Yue, X. Pei, B. Liu and X. Yan, Single-cell transcriptomic architecture and intercellular crosstalk of human intrahepatic cholangiocarcinoma, *J. Hepatol.*, 2020, **73**(5), 1118–1130.

149 Q. Liu, Y. Sun, H. Huang, C. Chen, J. Wan, L. Ma, Y. Sun, H. Miao and Y. Wu, Sirtuin 3 protects against anesthesia/surgery-induced cognitive decline in aged mice by suppressing hippocampal neuroinflammation, *J. Neuroinflammation*, 2021, **18**(1), 41.

150 P. Kongsuphol, H. H. Ng, J. P. Pursey, S. K. Arya, C. C. Wong, E. Stulz and M. K. Park, EIS-based biosensor for ultra-sensitive detection of TNF-α from non-diluted human serum, *Biosens. Bioelectron.*, 2014, **61**, 274–279.

151 F. Bhatti, D. Xiao, T. Jebagu, X. Huang, E. Witherspoon, P. Dong, S. Lei, J. Shen and Z. Wang, Semiconductive biocomposites enabled portable and interchangeable sensor for early osteoarthritis joint inflammation detection, *Adv. Compos. Hybrid Mater.*, 2023, **6**(1), 33.

152 D. Shi, C. Zhang, X. Li and J. Yuan, An electrochemical paper-based hydrogel immunosensor to monitor serum cytokine for predicting the severity of COVID-19 patients, *Biosens. Bioelectron.*, 2023, **220**, 114898.

153 C. Russell, A. C. Ward, V. Vezza, P. Hoskisson, D. Alcorn, D. P. Steenson and D. K. Corrigan, Development of a needle shaped microelectrode for electrochemical detection of the sepsis biomarker interleukin-6 (IL-6) in real time, *Biosens. Bioelectron.*, 2019, **126**, 806–814.

154 D. Najjar, J. Rainbow, S. Sharma Timilsina, P. Jolly, H. de Puig, M. Yafia, N. Durr, H. Sallum, G. Alter, J. Z. Li, X. G. Yu, D. R. Walt, J. A. Paradiso, P. Estrela, J. J. Collins and D. E. Ingber, A lab-on-a-chip for the concurrent electrochemical detection of SARS-CoV-2 RNA and anti-SARS-CoV-2 antibodies in saliva and plasma, *Nat. Biomed. Eng.*, 2022, **6**(8), 968–978.

155 Y. Song, R. Y. Tay, J. Li, C. Xu, J. Min, E. Shirzaei Sani, G. Kim, W. Heng, I. Kim and W. Gao, 3D-printed epifluidic electronic skin for machine learning–powered multimodal health surveillance, *Sci. Adv.*, 2023, **9**(37), eadi6492.